Draft version September 16, 2013
Preprint typeset using LaTeX style emulateapj v. 5/2/11



# THE $\kappa$ ANDROMEDAE SYSTEM: NEW CONSTRAINTS ON THE COMPANION MASS, SYSTEM AGE & FURTHER MULTIPLICITY

Sasha Hinkley[1,17], Laurent Pueyo[2,18], Jacqueline K. Faherty[3], Ben R. Oppenheimer[4], Eric E. Mamajek[5], Adam L. Kraus[6], Emily Rice[7,3], Michael J. Ireland [8,9], Trevor David[1], Lynne A. Hillenbrand[1], Gautam Vasisht[10], Eric Cady[10], Douglas Brenner[4], Aaron Veicht[4], Ricky Nilsson[4], Neil Zimmerman[11], Ian R. Parry[12], Charles Beichman[13], Richard Dekany[14], Jennifer E. Roberts[10], Lewis C Roberts Jr.[10], Christoph Baranec[14], Justin R. Crepp[15], Rick Burruss[10], J. Kent Wallace[10], David King[12], Chengxing Zhai[10], Thomas Lockhart[10], Michael Shao[10], Rémi Soummer[2], Anand Sivaramakrishnan[2], Louis A. Wilson[16]

*Draft version September 16, 2013*

## ABSTRACT

$\kappa$ Andromedae is a B9IVn star at 52 pc for which a faint substellar companion separated by 55$\pm$2 AU was recently announced. In this work, we present the first spectrum of the companion, "$\kappa$ And B," using the Project 1640 high-contrast imaging platform. Comparison of our low-resolution $YJH$-band spectra to empirical brown dwarf spectra suggests an early-L spectral type. Fitting synthetic spectra from PHOENIX model atmospheres to our observed spectrum allows us to constrain the effective temperature to $\sim$2000 K, as well as place constraints on the companion surface gravity. Further, we use previously reported $\log(g)$ and $T_{\rm eff}$ measurements of the host star to argue that the $\kappa$ And system has an isochronal age of 220$\pm$100 Myr, older than the 30 Myr age reported previously. This interpretation of an older age is corroborated by the photometric properties of $\kappa$ And B, which appear to be marginally inconsistent with other 10-100 Myr low-gravity L-dwarfs for the spectral type range we derive. In addition, we use Keck aperture masking interferometry combined with published radial velocity measurements to rule out the existence of any tight stellar companions to $\kappa$ And A that might be responsible for the system's overluminosity. Further, we show that luminosity enhancements due to a nearly "pole-on" viewing angle coupled with extremely rapid rotation is unlikely. $\kappa$ And A is thus consistent with its slightly evolved luminosity class (IV) and we propose here that $\kappa$ And, with a revised age of $220 \pm 100$ Myr, is an interloper to the 30 Myr Columba association with which it was previously associated. The photometric and spectroscopic evidence for $\kappa$ And B combined with our re-assesment of the system age implies a substellar companion mass of $50^{+16}_{-13}$ $M_{Jup}$, consistent with a brown dwarf rather than a planetary mass companion.

*Subject headings:* —planets and satellites: detection— stars: individual ($\kappa$ And)— techniques: high angular resolution— instrumentation: adaptive optics— instrumentation: interferometers— planetary systems.

## 1. INTRODUCTION

Recent observations of young stars in the solar neighborhood, employing high-contrast imaging techniques (e.g. Absil & Mawet 2010; Oppenheimer & Hinkley 2009) have begun to determine the frequency and orbital distributions of substellar and planetary-mass companions to nearby stars (Metchev & Hillenbrand 2009; Nielsen & Close 2010; Leconte et al. 2010; Vigan et al. 2012). Observing the youngest systems, in which substellar companions are still self-luminous during their initial contraction, reduces the still formidable challenge of overcoming the large brightness difference between the companion and the host star. Indeed, high-contrast observations in very young ($\sim$2-10 Myr) star forming regions have uncovered a handful of wide-separation planetary-mass companions (e.g. Chauvin et al. 2004; Lafrenière et al. 2008; Ireland et al. 2011, Kraus et al. *submitted*), although debate continues regarding the exact nature of these objects.

Further, some high contrast imaging surveys (e.g. Vigan et al. 2012; Oppenheimer et al. 2012; Rameau et al. 2013) have been targeting nearby field and moving group stars. Assigning ages for intermediate-mass, early-type stars is particularly challenging given the relative immaturity of this field compared to solar type stars for which many empirical age proxies are

[1] Department of Astronomy, Caltech, 1200 E. California Blvd, MC 249-17, Pasadena, CA 91125
[2] STScI, 3700 San Martin Drive, Baltimore, MD 21218, USA
[3] Department of Astronomy, Universidad de Chile Cerro Calan, Las Condes, Chile, USA
[4] Astrophysics Department, AMNH, Central Park West at 79th Street, New York, NY 10024, USA
[5] Department of Physics and Astronomy, University of Rochester, Rochester, NY 14627-0171, USA
[6] Harvard-Smithsonian CfA, 60 Garden St, Cambridge, MA 02140, USA
[7] College of Staten Island, CUNY, 2800 Victory Bvld, Staten Island, NY 10314, USA
[8] Department of Physics and Astronomy, Macquarie University, NSW 2109, Australia
[9] AAO, PO Box 296, Epping NSW 1710, Australia
[10] JPL, 4800 Oak Grove Dr., Pasadena CA 91109, USA
[11] MPIA, Knigstuhl 17, 69117 Heidelberg, Germany
[12] Institute of Astronomy, Cambridge CB3 0HA, UK
[13] NExScI, California Institute of Technology, Pasadena, CA 91125
[14] Caltech Optical Observatories, Pasadena, CA 91125, USA
[15] University of Notre Dame, Dept. of Physics, 225 Nieuwland Science Hall, Notre Dame, IN 46556, USA
[16] Washington University, St. Louis, MO, 63130
[17] NSF Fellow, email: shinkley@astro.caltech.edu
[18] Sagan Fellow

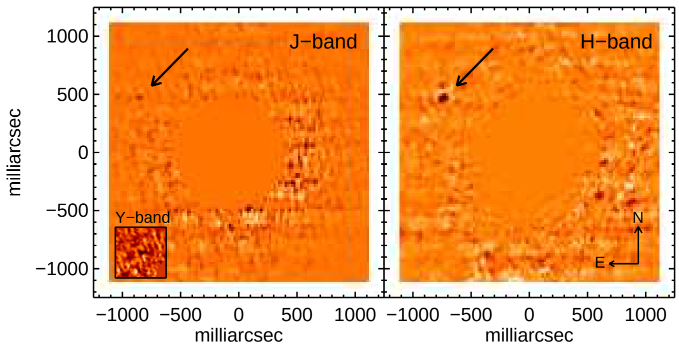


FIG. 1.— A post-processed image obtained on 23 December 2012 from the Project 1640 high contrast imaging platform showing the $\kappa$ And B companion at the upper left.

available. One such young, intermediate-mass field star, Kappa Andromedae (hereafter, "$\kappa$ And") is a B9IVn star located at 52 pc for which a planetary-mass companion, "$\kappa$ And B", was announced by Carson et al. (2013). Zuckerman et al. (2011a) claim that $\kappa$ And is a member of the 30 Myr Columba association and using this assumption, Carson et al. (2013) derive a mass of 12-13 $M_{Jup}$ for the companion. [1]

We begin with a discussion of the companion (§2), including a presentation of the first spectrum of this object (§2.1). Comparing our spectrum with empirical spectra of brown dwarfs (§2.2) indicates the spectrum of this object is consistent with spectra for an "intermediate age" ($\lesssim$300 Myr) low-gravity L1 brown dwarf, but similiarities with slightly later spectral type ($\sim$L4) field objects remain. In §2.3, we compare our data with synthetic model spectra of substellar objects to constrain the surface gravity and derive a best-fit $T_{\rm eff}\sim$2000K. Section 2.4 presents our analysis of the near-infrared photometry of $\kappa$ And B comparing its published $(J-K_s)$ color with the near-infrared colors for low-gravity $\gamma$ L-dwarfs for the early-L spectral type we derive. In §3, we review the properties of the host star, $\kappa$ And A. Using previously published log($g$) and $T_{\rm eff}$ data for $\kappa$ And A, we use isochronal analysis to present a revised system age (§3.2). In addition, we show that $\kappa$ And A is overluminous for a star with the originally assumed age of 30 Myr, suggesting substantial evolution away from the zero-age main sequence. Using aperture masking interferometry (§3.3), we place stringent limits on the presence of any stellar multiplicity that would be responsible for the overluminosity. We also show in §3.4 that a "pole-on" viewing angle, coupled with extremely rapid rotation, is unlikely for $\kappa$ And, which could also be responsible for the overluminosity. Finally, given the disparity between our 220 Myr derived age and the young 30 Myr age of the Columba Association with which it was previously associated, in §3.5 we re-examine the kinematics of the $\kappa$ And system and suggest that the $\kappa$ And may in fact be an interloper to Columba. Synthesizing this information, our re-assessment of the key parameters of this system implies a mass of $50^{+16}_{-13}$ $M_{Jup}$ for $\kappa$ And B, consistent with a brown dwarf rather than a planetary mass companion.

[1] It is worth noting that our choice to use "$\kappa$ And B" to refer to the companion should not be confused with the purported *stellar* companions "$\kappa$ And B" and "$\kappa$ And C" identified by Herschel (1831). We note that the Washington Double Star (WDS) catalog refers to the companion reported in Carson et al. (2013) as "$\kappa$ And Ab", since it is the fourth component of the $\kappa$ And ABC system to be discovered. However, as we describe in the appendix, it is exceedingly unlikely that the *stellar* components "$\kappa$ And B" and "C" identified by Herschel (1831) are physical components of the $\kappa$ And system. Nonetheless, they are listed as such in the WDS. We choose to use "$\kappa$ And B" instead of "Ab" to remain consistent with Carson et al. (2013).

TABLE 1
DERIVED PROPERTIES FOR $\kappa$ AND B

| Parameter | Value | Units | Reference |
|---|---|---|---|
| $T_{\rm eff}$ | 2040±60 | K | This work (§2.3) |
| Spectral Type | L1±1 | | This work (§2.1) |
| Mass | $50^{+16}_{-13}$ | $M_{Jup}$ | This work (§2.3) |
| log($g$) | $4.33^{+0.88}_{-0.79}$ | | This work (§2.3) |
| Age | 220±100 | Myr | This work (§3.2) |

NOTE. —

## 2. PROPERTIES OF THE SECONDARY: $\kappa$ AND B

In this section, we present new spectrophotometry of $\kappa$ And B which is compared with empirical and synthetic spectra of substellar objects, as well as an analysis of the near-infrared colors of the object.

### 2.1. *Spectroscopy from 0.9 - 1.8 $\mu m$*

We imaged the $\kappa$ And system on UT 2012 December 23 using "Project 1640" (Hinkley et al. 2011c; Oppenheimer et al. 2012) on the 200-in Hale Telescope at Palomar Observatory. Project 1640 is a coronagraph integrated with an integral field spectrograph ("IFS", Hinkley et al. 2008) covering the $YJH$-bands. This instrument ensemble is mounted on the Palomar "PALM-3000" AO system (Dekany et al. 1998; Roberts et al. 2012a), which in turn is mounted at the Cassegrain focus of the Hale Telescope. In addition, the system uses an internal wave front calibration interferometer (e.g. Wallace et al. 2004; Zhai et al. 2012) for reducing non-common path wave front errors internal to the instrument ensemble, thereby boosting performance at small angular separations.

Starting at an airmass 1.02, sixteen Project 1640 multi-spectral images were obtained, each with exposure time of 183s. The star was placed behind the coronagraphic mask, the PALM-3000 AO control loops were locked, and additional corrective wave front sensor offsets were applied to the PALM-3000 AO system from the wave front calibration interferometer, thus minimizing the halo of correlated speckle noise. To alleviate the inherent uncertainty in the position of the occulted star in coronagraphic images (e.g. Digby et al. 2006), the position of the star was determined by using a set of fiducial reference spots created by a physical pupil plane grid in the Project 1640 coronagraph (Sivaramakrishnan & Oppenheimer 2006; Marois et al. 2006b).

The Project 1640 data reduction pipeline is described in Zimmerman et al. (2011). To convert the image data counts obtained by the spectrograph to physically meaningful quantities, the counts in a Project 1640 pupil plane image of the $\kappa$ And system were measured with the star moved off the coronagraphic mask obtained shortly after the science observations. In this configuration, the

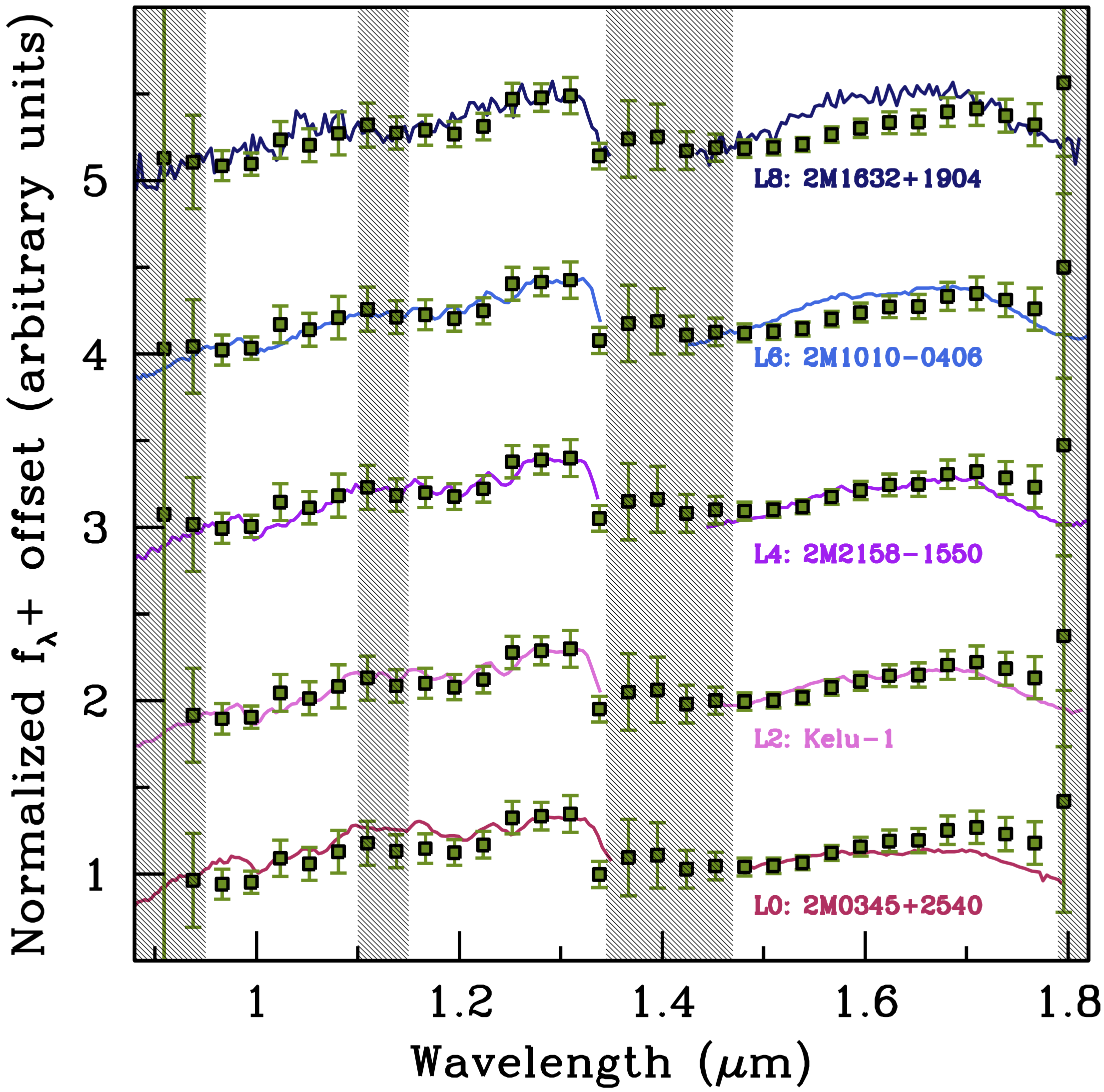


FIG. 2.— Comparison of Project 1640 spectra of $\kappa$ And B (points) with field brown dwarf standards ranging from L0 to L8 taken from Kirkpatrick et al. (2010). Each spectrum has been offset arbitrarily for clarity, although no other offsets of any kind have been applied to either the template spectra or the P1640 data. The shaded regions indicate spectral regions where telluric water absorption is strong.

entire field of view of the pupil plane is uniformly illuminated. Comparing the counts measured in each channel in the data cube with the actual flux value from an empirical spectrum for a B9 star from the Pickles Stellar Spectral flux library (Pickles 1998) provides a relation of data counts in the science camera to physical units of flux density.

Extracting a spectrum of an object such as $\kappa$ And B is challenging due to the $\sim 10^4$ contrast ratio between it and the host star at only $1''$. The single largest hindrance to extraction of high signal-to-noise spectra is the quasi-static speckle noise in the image focal plane (Racine et al. 1999; Marois et al. 2000; Hinkley et al. 2007). For objects with brightness greater than, or comparable to the speckle noise halo (e.g. Hinkley et al. 2010; Zimmerman et al. 2010; Hinkley et al. 2011b; Pueyo et al. 2012b; Hinkley et al. 2013), evaluation of companion spectra can be performed with conventional aperture photometry. However, for objects with higher contrast such as $\kappa$ And B or HR 8799 (Oppenheimer et al. 2013), an IFS can improve sensitivity through the suppression of this quasi-static speckle noise in the image (Crepp et al. 2011; Pueyo et al. 2012a).

To reduce the effects of quasi-static speckle noise in our multi-spectral images, we use speckle suppression techniques based on the principle component analysis algorithm outlined in Soummer et al. (2012). This method uses a basis of eigenimages created by a Karhunen-Loève transform of Point Spread Function (PSF) Reference images to perform the PSF subtraction, and is amenable to point source forward modelling (Pueyo et al *in prep.*). Applications of this method have been demonstrated for the directly imaged planets in the HR 8799 system (Oppenheimer et al. 2013). Figure 1 shows three images from the Project 1640 IFS subsequent to our speckle sup-

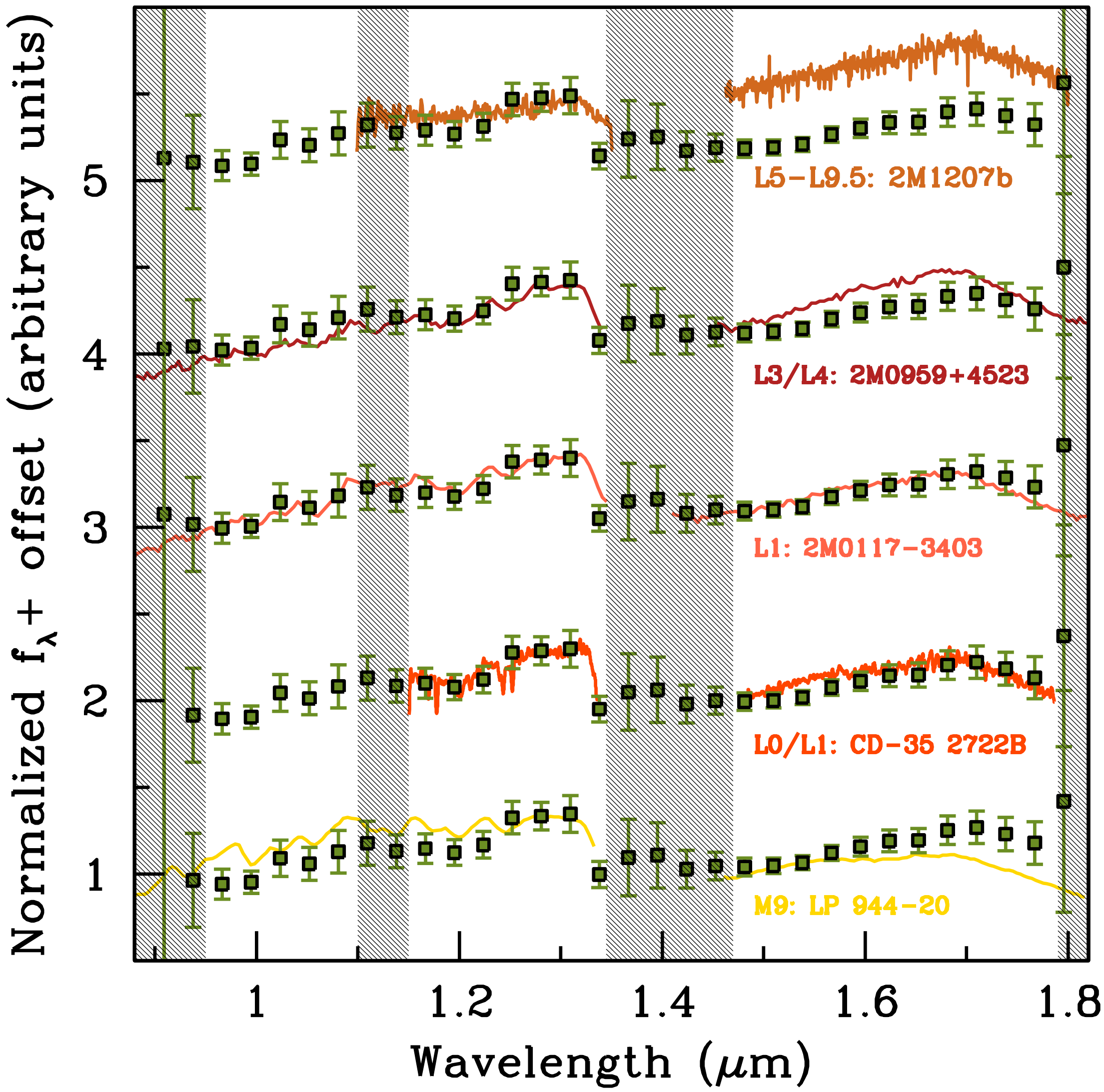


Fig. 3.— Comparison of the Project 1640 spectra of $\kappa$ And B (green points) with several young and intermediate age L-dwarfs ranging from L1 to later than L5 (see text for details). Also shown is an M9 object presented in Burgasser et al. (2008) as well as the very young 2M1207b (Patience et al. 2010). The best match empirical spectra to the Project 1640 data is the $\sim$50-150 Myr L1$\pm$1 object 2M0117-3403 (Faherty et al. *in prep*), which has a $(J-H)$=0.97$\pm$0.05 color, consistent with the published value of 0.91 $\pm$ 0.1 from Bonnefoy et al. (2013b). Each spectrum has been offset arbitrarily for clarity, although no other offsets of any kind have been applied to either the empirical spectra or the Palomar data. The shaded regions roughly indicate spectral regions where telluric water absorption is strong.

pression post-processing corresponding the $Y$, $J$, and $H$-band central wavelengths.

As with any form of PSF subtraction (e.g. classical ADI, LOCI, Marois et al. 2006a; Lafrenière et al. 2007), the performance of the algorithm centers on robust co-alignment of the PSF reference images. To align our reference images, we perform an initial alignment based on the fiducial astrometric reference spots in the data, and perform a subsequent sub-pixel cross-correlation using the image speckles. To verify that the extraction of spectra is robust and that flux is not significantly depleted from the $\kappa$ And B source, we execute a parameter space search as follows: we use 16 different geometries near the location of the companion (these include varying the size of the search zone and the radial exclusion parameter necessary to mitigate cross talk between nearby spectral channels), and vary the number of eigenmodes in the PSF subtraction from 1 to 130. This parameter search results in $\sim$2000 spectra for the $\kappa$ And B companion. From these $\sim$2000 spectra, we discard any spectra for which a) the astrometric position of the companion is not consistent between wavelength channels; b) a sharp flux drop is detected with a small change in the number of modes. Eliminating reduced spectra in case a) ensures that the extraction is not biased by residual speckle noise (should a speckle have some overlap with the companion then it will yield a wavelength dependent astrometric bias). A sharp drop in flux over a small number of modes indicates that too many eigenmodes are being used, thus in case b) we eliminate spectra corresponding to overly aggressive PSF subtractions. Finally we further trim this subset by only keeping the spectra that exhibit a *local* SNR > 3

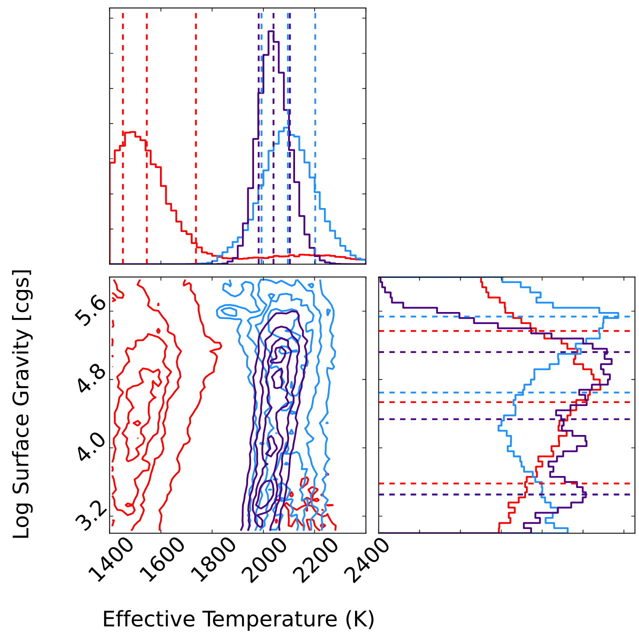


FIG. 4.— Posterior distributions for the MCMC fits of synthetic spectra to the Project 1640 data shown in Figure 5. The figure uses the same color scheme as Figure 5. Namely, the blue distributions show the results to the fits of only the $Y$ and $J$ portions of the spectra, red corresponds to $H$-band, and purple is the full spectral range $YJH$. The best-estimate for each parameter correspond to the 50% quantile. One dimensional representations of the marginalized temperature and surface gravity posterior distributions are shown at the top and right, respectively, with best-estimate, and 68% confidence intervals marked by the dashed lines.

for all wavelengths in the band of interest (either $Y + J$ or $H$). This procedure leads to ∼40 high quality spectra for the companion. The mean of these values comprises the spectral points plotted in Figures 2 and 3 (green individual points), and the error bars denote the standard deviation of these ∼40 spectra, plus the uncertainty associated with the pupil-plane spectral calibration added in quadrature.

### 2.2. *Comparison with Empirical Brown Dwarf Spectra*

Figure 2 shows the $YJH$-band spectro-photometry from Project 1640 for $\kappa$ And B. Overlaid with the spectra in Figure 2 are empirical spectra for field-age "standard" objects taken from Kirkpatrick et al. (2010), ranging from spectral type L0 to L8. The empirical spectra are normalized such that they match the Project 1640 flux at 1.28 $\mu$m, and the figure identifies three regions near 1.1, 1.4, and 1.8 $\mu$m where telluric water absorption is particularly strong. Assuming a surface gravity value appropriate for dwarf-like objects, the Palomar data show a best match to the mid-L spectral types. Specifically, as demonstrated in Table 2, a $\chi^2$ goodness-of-fit metric reveals a best-fit to the L4 field object 2MASS J21580457-1550098.

However, as we discuss in §3.2, the $\kappa$ And system likely has an age of 220±100 Myr, significantly younger than typical field ages (∼few Gyr). Thus, comparison with spectra of L-dwarfs with known indicators of youth may be more appropriate. Figure 3 shows our $YJH$-band spectro-photometry along with several young and intermediate age substellar objects ranging from the very young (∼10 Myr) object 2MASS J12073346-3932539b (hereafter, 2M1207b) (Patience et al. 2010) to the mid-late young L-dwarf 2M0959 (∼150 Myr, Faherty et al. *in prep*), and LP 944-20, a ∼300 Myr late-M dwarf (Burgasser et al. 2008). Several of these objects are discussed in §2.4 and shown in Figure 8, as well. Among the young objects, the best fitting ($\chi^2$=0.76) synthetic spectrum to our data is 2MASS J01174748-3403258 (hereafter, 2M0117-3403), a L1±1 "$\beta$" intermediate-gravity brown dwarf (Allers & Liu 2013). Indeed, the best fit template spectrum of the L1± object 2M0117 to our $\kappa$ And B spectra has a $(J - H)$= 0.97±0.05 well matched to that of $\kappa$ And B. Thus, comparing to objects with ages more appropriate to $\kappa$ And implies a slightly earlier spectral type object (L1: 2000±200K, e.g. Kirkpatrick 2005) than would be inferred for a later type field age L4 object (1700-1900K).

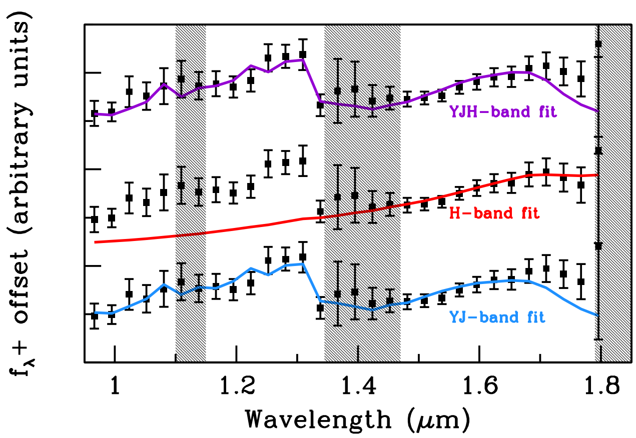


FIG. 5.— The best fit synthetic PHOENIX models (Hauschildt et al. 1997; Barman et al. 2001; Allard et al. 2001) to the Project 1640 spectra. The models have been fit using the methods of Roberts et al. (2012b) and Rice et al. (*in prep*). The lower curve (blue) is the best-fit synthetic model to only the $Y$ and $J$-band Project 1640 points, while the middle curve (red) shows the best fit synthetic model for $\kappa$ And B to only the $H$-band spectral points (1.45-1.80 $\mu$m). The top curve (purple) reflects the best fit values for all the $YJH$-bands simultaneously. Figures 4 and 6 use the same color scheme.

The comparable quality of fits to empirical spectra of the intermediate-gravity L1 object as well as the L4 field object prevents us from placing extremely strong constraints on the spectral type of $\kappa$ And B. Given the relatively low spectral resolution and finite wavelength coverage ($YJH$-bands) Project 1640 data, these data may only be able to discern a range of spectral types for this companion (e.g. ∼L1-L4). Further, discerning gravity-sensitive features from these data may be challenging, especially at high contrast, and when heavy contamination from speckle noise is present. Observations of targets with well known gravity features may be needed to calibrate the strength of gravity effects in the data. Nonetheless, our best match to the low-gravity young object 2M0117 is likely a point of consistency with our revised 220 Myr age of the primary (§3.2). We thus adopt a conservative estimate of L1±1 for $\kappa$ And B. As we show below, fitting synthetic models to our spectra give temperatures consistent with an L1±1 object

TABLE 2
$\chi^2$ Goodness of Fit values for Brown Dwarf Template Spectra

| | Object | Spectral Type | $\chi^2$ |
|---|---|---|---|
| Young Brown Dwarfs: | | | |
| | LP 944-20 | M9 | 1.91 |
| | CD-35 2722 B | L0-L1 | 4.03 |
| | 2M 0117-3403 | L1 | 0.76 |
| | 2M 0959+4523 | L3-L4 | 1.97 |
| | 2M 1207b | L5-L9.5 | >40 |
| Field objects: | | | |
| | 2M 0345+2540 | L0 | 1.81 |
| | Kelu-1 | L2 | 0.96 |
| | 2M 2158-1550 | L4 | 0.65 |
| | 2M 1010-0406 | L6 | 1.91 |
| | 2M 1632+1904 | L8 | 4.15 |

Note. —

(§2.3), and color-magnitude diagram analysis supports the L1±1 identification (§2.4, Figure 7).

### 2.3. *Comparison with Synthetic Spectra*

To directly constrain the physical properties of this object, we compare (e.g. Roberts et al. 2012b, , Rice et al. *in prep*) the observed P1640 spectrum to a grid of synthetic spectra from the PHOENIX models (Hauschildt et al. 1997; Barman et al. 2001; Allard et al. 2001). The model atmospheres cover $T_{\rm eff}$ = 1400K to 4500K and log($g$)= 3.0-6.0 in intervals of 50K and 0.1 dex at solar metallicity using the *dusty* version of dust treatment and are described in more detail by Rice et al. (2010) and Roberts et al. (2012b). The adopted best-fit parameters are the 50% quantile values of the $10^6$ link posterior distribution functions from a Markov chain Monte Carlo (MCMC) analysis that interpolates between calculated synthetic spectra, creating an effectively continuous grid of models.

We use three different spectral ranges: 0.9 - 1.32$\mu$m ($YJ$-bands), 1.47-1.78$\mu$m ($H$-band), and the full range 0.9 - 1.78$\mu$m ($YJH$-bands) for the spectral comparison. We exclude the four points occupying the water band separating the $J$ and $H$-bands (∼1.4$\mu$m) as well as the final $H$-band point near 1.8$\mu$m, but we include the two points in the water band between the $Y$ and $J$-bands, since their uncertainties are comparable with points in the bandpasses. Figure 5 shows the three best fit synthetic spectra and their input physical parameters for each spectral region, plotted over the entire observed spectrum. The fit to the full set of data ($YJH$-bands) is the best overall and has similar parameters (2040K$^{+58}_{-64}$, log($g$)=4.33$^{+0.88}_{-0.79}$, ±68% confidence intervals ) as the $YJ$-band only fit (2096K$^{+103}_{-106}$, log($g$)=4.65$^{+1.20}_{-0.89}$). As Figure 5 shows, the fit to only the $H$-band data significantly underpredicts several flux points in $YJ$-bands, producing a temperature ∼1550K, and we regard this as physically unreasonable. Figure 4 shows the posterior distributions for fits for each of the three cases, along with the margnalized one-dimensional posterior distributions for each fitting parameter.

In Figure 6 we compare the best-fit $T_{\rm eff}$ and log($g$) values to parameters predicted by DUSTY00 models from Chabrier et al. (2000) and Baraffe et al. (2002) for ages ranging from 1 Myr to 5 Gyr, and masses ranging from 8 $M_{Jup}$ to 75 $M_{Jup}$. The uncertainties on the best-fit

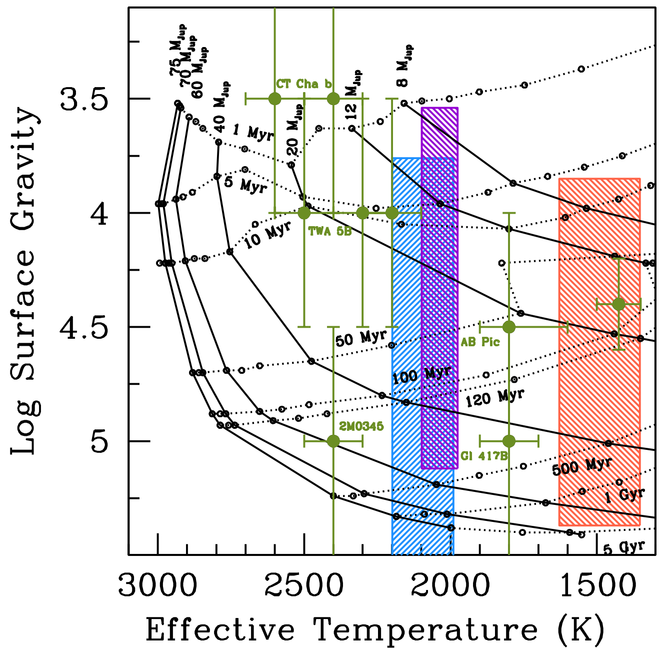


Fig. 6.— The best fit log($g$) and $T_{\rm eff}$ values for $\kappa$ And B derived by comparing to sythetic spectra using the methods of Rice et al. (2010). The red box identifies the ±68% confidence intervals of the fit in both temperature and gravity to only the Project 1640 H-band spectral points (1.45-1.80 $\mu$m) for $\kappa$ And B, the blue region indicates the ±68% confidence intervals for the $YJ$-bands, while the purple region reflects the ±68% confidence intervals for all the Project 1640 wavelengths simultaneously ($YJH$-bands). The best fit synthetic specta are shown in Figure 5, and the posterior distributions for our MCMC fitting procedure are shown in Figure 4. Also shown are age/mass isochrones from the DUSTY00 models from Chabrier et al. (2000) and Baraffe et al. (2002). The gray circular points indicate the log($g$) and $T_{\rm eff}$ values from several young, low mass M and L-type objects taken from Bonnefoy et al. (2013a) and Bowler et al. (2013).

physical parameters for $\kappa$ And B represent the width of the distribution of the $10^6$-link Markov chain values marginalized over the other parameter, as described in Roberts et al. (2012b, Rice et al. *in prep.*). Also shown are the locations in log($g$) versus $T_{\rm eff}$ space of several young M and L-type objects taken from Bonnefoy et al. (2013a) and Bowler et al. (2013).

The locations of the $YJ$-band and $YJH$-band best fit $T_{\rm eff}$ values (2000-2100K) and their uncertainties are consistent with an L1±1 spectral type (e.g. Kirkpatrick 2005; Stephens et al. 2009). However, the constraints on the surface gravity for $\kappa$ And B still permit a wide range of ages, from very young to several hundred Myr. However, the range still includes our revised age of 220±100 Myr. Indeed, low resolution spectral fits to known young very low mass objects presented in Rice et al. (*in prep.*) also suggest surface gravities higher than would be expected for the ∼10–100 Myr ages, possibly indicating the inadequacy of the simplified dust treatment of the *dusty* PHOENIX model atmospheres in recreating the emergent spectra of young, very low mass objects.

### 2.4. *Near-infrared Luminosity and Colors*

Combining luminosity with NIR color has emerged as a potentially powerful lever for deciphering age properties of brown dwarfs and giant planets. For example, normal field L dwarfs typically have ($J - K_s$)=1.3-

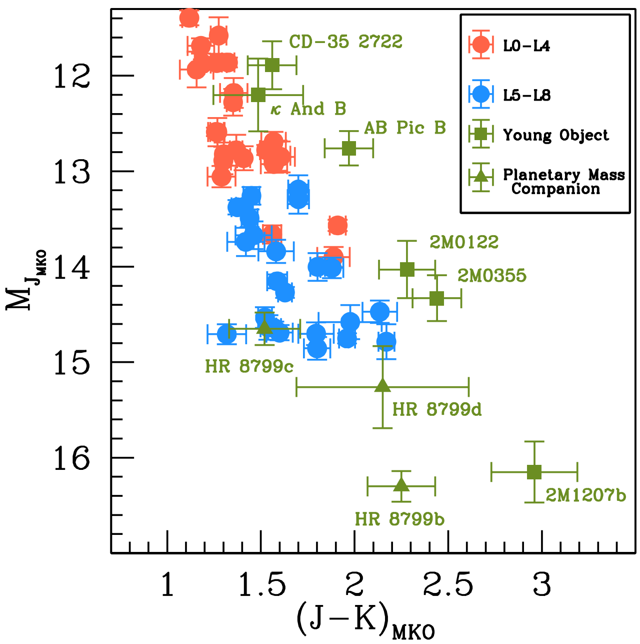


FIG. 7.— The near-infrared color magnitude diagram for well-studied field and young L-type brown dwarfs as well as planetary mass companions. Absolute magnitudes were derived from parallaxes reported in Faherty et al. (2012) and Dupuy & Liu (2012). The placement of $\kappa$ And B is consistent with an L1±1 spectral type. We also show comparably young L dwarfs 2M0355, AB Pic b, and CD-35 2722B, and 2M0122-2439B (See also Figure 3 and Figure 8).

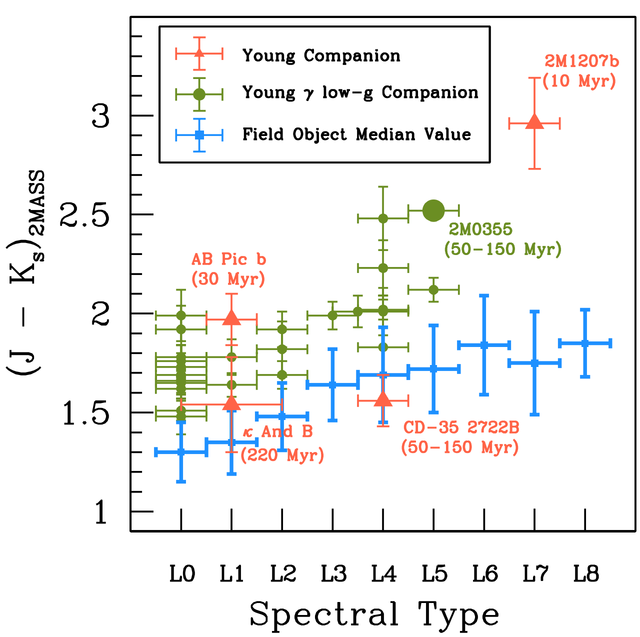


FIG. 8.— 2MASS $(J - K_s)$ color versus spectral type for field L0-L9 dwarfs. Mean colors of normal (excluding subdwarfs and suspected young) objects are displayed as blue points with error bars. Low surface gravity $\gamma$ L-dwarfs (denoted by "$\gamma$ Low-G") are the grey points with the most extreme, 2M0355, highlighted. Companion L dwarfs are shown as red triangles. Using the $(J-K_s)$ color as a coarse age discriminator, $\kappa$ And B is evidently older than the very young objects such as AB Pic b, 2M1207b, and 2M0355, but still possibly consistent with the population of $\gamma$ L-dwarf.s

1.8, while the $\gamma$ low-gravity sources are ∼0.3-0.6 magnitudes redder than the median for their respective spectral types (Figure 8). When one combines the absolute $JHK$ magnitudes of the $\gamma$ sources and compares them to equivalent spectral type targets, one finds they are not just redward but also up to 1.0 mag underluminous (Faherty et al. 2012, 2013) in the NIR. The same trend has been cited in directly imaged giant exoplanet studies (e.g. 2M1207b and HR8799b; Chauvin et al. 2004; Marois et al. 2010). Figures 7 and 8 show the properties of $\kappa$ And B compared to field brown dwarfs as well as four well studied, young L dwarfs: AB Pic B, CD-35 2722 B, 2M0355+1133, and 2M1207 B (Chauvin et al. 2005; Wahhaj et al. 2011; Faherty et al. 2013; Chauvin et al. 2004). Several of these young L-dwarfs are used for comparison in Figure 3 (§2.1).

As shown in Figure 7, $\kappa$ And B has a comparable absolute magnitude to L0-L4 dwarfs, including the planetary mass object AB Pic B (SpT L1; Bonnefoy et al. 2013). However, AB Pic B is redder than the "main sequence" of L and T dwarfs as well as $\kappa$ And B, and forms a sequence with comparably young sources 2M1207b, and 2M0355. Indeed, Figure 8 shows that $\kappa$ And B is consistent with the median $(J - K_s)$ colors of field L-dwarfs, and is marginally inconsistent with the young $\gamma$ low-gravity objects. The luminosity alone rules out ∼mid to late spectral types as the lower temperatures would make $\kappa$ And B significantly overluminous. This suggests an earlier spectral type, consistent with the L1±1 spectral type derived in §2.2.

## 3. PROPERTIES OF $\kappa$ AND A

In §2 we presented spectroscopic and photometric evidence that the companion to $\kappa$ And is more consistent with an object that is older and higher mass than the young (30 Myr), and low mass (12-14 $M_{Jup}$) that has been claimed in the literature. In this section, we present further constraints on the age of the system through an analysis of fundamental properties of the host star.

### 3.1. *Stellar Parameters*

$\kappa$ And A is a V = 4.138 ± 0.003 mag (Mermilliod 1997) B9IVn (Cowley et al. 1969; Garrison & Gray 1994) star at distance 51.6 ± 0.5 pc ($\varpi$ = 19.37 ± 0.19 mas; van Leeuwen 2007). The "n" in the spectral type signifies that it is a fast rotator, however its $v\sin i$ (150 km s$^{-1}$; Abt et al. 2002) is not unusual for field B9 stars (Kraft 1967). At this distance, results from reddening surveys suggest that the star should be negligibly reddened ($E(b-y) < 0.02$ mag ; Reis et al. 2011).

Several lines of evidence point to a lower surface gravity for $\kappa$ And A compared to what would be expected of a ∼30 Myr-old star. Early indications of a luminosity class different than the dwarf categorization were presented by Cowley et al. (1969), and later by Cucchiaro et al. (1977), whose ultraviolet line analysis led to classification of $\kappa$ And A as "gB9", indicating a surface gravity more indicative of giants rather than dwarf stars. Thereafter, fitting of atmospheric models to ultraviolet photometry by Malagnini et al. (1983) derived a surface gravity of $\log(g) = 3.69$ − lower than the $\log(g) \simeq 4.2$-4.5 value typical for luminosity class V stars. Further, surface gravity estimates of $\log(g)$ = 4.17, 4.10, 3.97, 3.87, and 3.78 were estimated by

Allende Prieto & Lambert (1999), Fitzpatrick & Massa (2005), Prugniel et al. (2007), Wu et al. (2011), and Bonnefoy et al. (2013b) respectively. Taken as a group, these values are more commensurate with luminosity class IV than typical class V dwarf stars.

As a demonstration of this, Figure 9 shows these values from the literature in a log($g$) versus $T_{\rm eff}$ diagram. This figure also shows a region of log($g$) space (shaded band) spanned by a compendium of spectroscopic surface gravity measurements for subgiant standard stars from the PASTEL database (Soubiran et al. 2010)[19]. An assessment of the quality of the spectroscopic standards was made: those that showed the most consistency in the literature, and/or had the best pedigrees were used. This band has a width of ±0.19 dex, as determined by the 1$\sigma$ variation of the log($g$) measurements from the subgiant standards. This scatter reflects a mix of differences amongst spectroscopic log($g$) values published for a single subgiant standard star, and standard-to-standard differences. Given the heterogeneity of the data, we do not attempt to disentangle which effects dominate, but the data seem to suggest that ±0.2 dex rms accuracy in log($g$) is a reasonable lower limit on the predictive power of luminosity class IV to predict surface gravity. Fitting a fifth-order polynomial to the log($g$)measurements (spanning spectral types B0 to K1) predicts a log($g$)=3.75±0.19 for a B9IV star.

$\kappa$ And's effective temperature ($T_{\rm eff}$) has been estimated as 10594 K (Prugniel et al. 2007), 10733 ± 247 K (Wu et al. 2011), 10839 ± 200 K (Zorec & Royer 2012), 10965 K (Allende Prieto & Lambert 1999), 11246 K (Grosbol 1978), 11240 K (Malagnini et al. 1983; Morossi & Malagnini 1985), 11310 K (Napiwotzki et al. 1993), 11361 ± 66 K (Fitzpatrick & Massa 2005), 11535 K (Westin 1985). Arguably the most comprehensive analysis is by Fitzpatrick & Massa (2005), who fit Kurucz ATLAS9 model synthetic spectra to optical/infrared photometry and *IUE* ultraviolet spectra. Fitzpatrick & Massa (2005) derived extremely well-constrained stellar parameters of $T_{\rm eff}$ = 11361 ± 66 K, [Fe/H] = -0.36 ± 0.09 dex, radius 2.31 ± 0.09 $R_\odot$, and spectroscopic surface gravity log($g$) = 4.10 ± 0.03 dex. Given their adopted distance based on the original Hipparcos catalog ($d$ = 52.0 ± 1.6 pc), their parameters imply an angular diameter of 413 ± 16 $\mu$as (of which ±13 $\mu$as is due to the distance error, with presumably ±10 $\mu$as coming from the uncertainty in the bolometric flux). Using the revised Hipparcos parallax of $\varpi = 19.37 \pm 0.19$ mas ($d$ = 51.63 ± 0.51 pc; 1% error), we update the luminosity estimate from Fitzpatrick & Massa (2005) to $\log(L/L_\odot) = 1.895 \pm 0.024$ dex.

More accurate determinations of luminosity and $T_{\rm eff}$ could easily be made if the inclination of $\kappa$ And were to be determined through interferometry (e.g. Monnier et al. 2012), enabling stellar parameters to be computed that are not biased by our unknown viewing angle of this rapid rotator. We discuss aspects of the star's inclination in greater detail in § 3.4.

## 3.2. *Age*

### 3.2.1. *Chemical Composition*

[19] http://vizier.u-strasbg.fr/viz-bin/VizieR?-source=B/pastel

TABLE 3
Stellar Parameters

| (1) Parameter | (2) Value | (3) Units | (4) Ref. |
|---|---|---|---|
| Parallax($\varpi$) | 19.37 ± 0.19 | mas | 1 |
| Distance(1/$\varpi$) | 51.63 ± 0.51 | pc | 1 |
| $\mu_{\alpha *}$ | 80.73 ± 0.14 | mas yr$^{-1}$ | 1 |
| $\mu_\delta$ | -18.70 ± 0.15 | mas yr$^{-1}$ | 1 |
| $v_R$ | -12.7 ± 0.8 | km s$^{-1}$ | 2 |
| U | -11.5 ± 0.3 | km s$^{-1}$ | this work |
| V | -20.1 ± 0.5 | km s$^{-1}$ | this work |
| W | -5.9 ± 0.6 | km s$^{-1}$ | this work |
| $m_V$ | 4.138 ± 0.003 | mag | 3 |
| $M_V$ | 0.574 ± 0.037 | mag | 4 |
| $T_{\rm eff}$, | 11361 ± 66 | K | 5 |
| $v$sin$i$ | 150 | km s$^{-1}$ | 6 |
| $\log(L/L_\odot)$ | 1.895 ± 0.024 | dex | 7 |
| Radius | 2.29 ± 0.06 | $R_\odot$ | 7 |
| Mass | $2.8^{+0.1}_{-0.2}$ | $M_\odot$ | this work |
| Age | 220 ± 100 | Myr | this work |

Note. — References: (1) van Leeuwen (2007), (2) Gontcharov (2006), (3) Mermilliod (1997), (4) this paper, calculated using data in this table, (5) Fitzpatrick & Massa (2005), (6) Abt et al. (2002), (7) calculated using values from Fitzpatrick & Massa (2005), updated using the new Hipparcos parallax from van Leeuwen (2007).

The chemical composition of $\kappa$ And is worth briefly discussing before trying to constrain its age using modern stellar evolutionary tracks. Subsolar photospheric metallicities of [Fe/H] = -0.40 (Prugniel et al. 2007), -0.45 (Katz et al. 2011), -0.36 (Fitzpatrick & Massa 2005), and -0.32 ± 0.15 (Wu et al. 2011) have been reported for $\kappa$ And. However, nearby, young (<200 Myr) open clusters and in the solar vicinity have [Fe/H] ∼ 0.0 with rms scatter ∼0.1 dex (e.g. Chen et al. 2003), as do the nearest star-forming regions (<10 Myr) and young stellar associations (Santos et al. 2008; Viana Almeida et al. 2009). If $\kappa$ And has kinematics consistent with a local origin, it is highly unlikely that the bulk composition of $\kappa$ And would vary significantly from solar.

For the Columba association, to which $\kappa$ And purportedly belongs, the only stars from published membership lists (Torres et al. 2008; Malo et al. 2013; Zuckerman et al. 2011b; Zuckerman & Song 2012) with spectroscopic metallicity ([Fe/H]) estimates published in the PASTEL compendium of stellar atmospheric parameters (Soubiran et al. 2010) are HD 984 (0.09; Valenti & Fischer 2005), HD 31647 (-0.12; Hill 1995), HD 39206 (0.06; Lemke 1989), and HD 40216 (0.00; Tagliaferri et al. 1994). Hence, thus far, Columba members have spectroscopic metallicities consistent with being approximately solar (mean [Fe/H] = 0.01 ± 0.05), and the spectroscopic [Fe/H] estimates for $\kappa$ And would appear to make the star chemically peculiar if it is truly associated with Columba.

Even *if* the bulk composition of $\kappa$ And is as metal poor as the spectroscopic estimates listed above ([Fe/H] = -0.32 to -0.45) indicate, this would only conspire to make the star systematically older when comparing to evolutionary tracks. In what follows, we assume that $\kappa$ And has solar bulk composition, similar to other very young stars in the solar vicinity. However, we also evaluate the age assuming a lower metallicity.

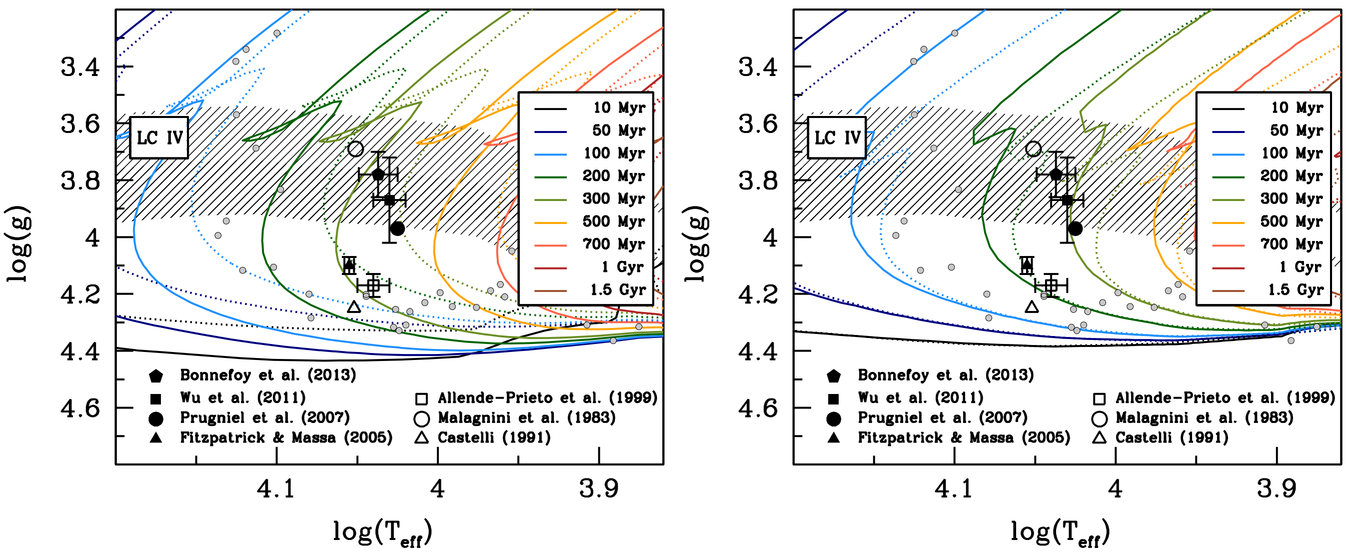


FIG. 9.— Previously published (see §3.2) determinations of $T_{\rm eff}$ and log($g$) for $\kappa$ And (large points) are compared with Pleiades members as discussed by David et al. (2014, *in prep*). *Left:* overlaid are the PARSEC isochrones of Bressan et al. (2012). The solid isochrones are for a metallicity of [M/H]=-0.36, the value for $\kappa$ And determined by Fitzpatrick & Massa (2005). The dashed isochrones are for solar metallicity. The isochrone ages include the pre-main sequence evolution timescales. All of the published determinations of $T_{\rm eff}$ and log($g$) for $\kappa$ And are consistent with an isochrone age > 200 Myr in the sub-solar metallicity case and an age > 50 Myr in the solar metallicity case. The shaded band labeled "LC IV" identifies the range of spectroscopic log($g$) measurements occupied by subgiant standard stars taken from the PASTEL data base (see text). *Right:* The solid curves are isochrones of Ekström et al. (2012) computed from stellar evolutionary models that start on the ZAMS with a rotation rate of $v_{rot}/v_{crit} = 0.4$. The dashed curves are isochrones computed from stellar evolutionary models with zero rotation. All of the published determinations of $T_{\rm eff}$ and log($g$) are consistent with an isochrone age > 100 Myr for $\kappa$ And, with several being consistent with ∼200 Myr.

#### 3.2.2. *log(g) versus $T_{\rm eff}$ Analysis*

As originally presented at IAU Symposium 299 in Victoria, BC on June 3, 2013, Figure 9 shows the log($g$) and $T_{\rm eff}$ values previously listed in the literature plotted along with two sets of isochrones for log($g$) and $T_{\rm eff}$. The left plot shows the PARSEC isochrones of Bressan et al. (2012) for two cases: a metallicity of [M/H]=-0.36, the value for $\kappa$ And determined by Fitzpatrick & Massa (2005), as well as solar metallicity. The isochrone ages include the pre-main sequence evolution timescales. All of the published determinations of $T_{\rm eff}$ and log($g$) for $\kappa$ And are consistent with an isochrone age > 200 Myr in the sub-solar metallicity case and an age > 50 Myr in the solar metallicity case.

The right panel of Figure 9 shows the isochrones taken from Ekström et al. (2012). These models are particularly applicable as they take the effects of stellar rotation into account. Indeed, Carson et al. (2013) use the work of Ekström et al. (2012) to derive a stellar mass. Figure 9 shows the isochrones for a rotation rate of $v_{rot}/v_{crit} = 0.4$ (See 3.2.3), as well as those for zero rotation. All of the published determinations of $T_{\rm eff}$ and log($g$) are consistent with an isochrone age > 100 Myr for $\kappa$ And, and several values are consistent with the 200 Myr isochrone. Further, for both plots, these literature points are located in a region of the log($g$) versus $T_{\rm eff}$ diagram where the isochrones are unambiguously well separated.

Also shown in Figure 9 are several log($g$)and $T_{\rm eff}$ values taken for individual members of the Pleiades from the $uvby\beta$ analysis of David et al. (2014, *in prep.*). Each of these points have had an individual $v \sin i$ rotation correction factor applied to them to account for the rotation and inclination effects discussed above. These points show good agreement with the solar metallicity 100 Myr tracks (blue dotted curve), appropriate for Pleiades-age objects.

By combining the spectroscopically-constrained parameters $T_{\rm eff}$ and log($g$) alone, and comparing the values to modern stellar evolutionary models, we infer that the age of $\kappa$ And is almost certainly in the range ∼50-400 Myr. The well-constrained combination of $T_{\rm eff}$ and log($g$) estimated by Fitzpatrick & Massa (2005) for $\kappa$ And A is consistent with age ∼300 Myr for subsolar composition ([M/H] = -0.36) and age ∼180 Myr for solar composition. Using the rotating and non-rotating tracks of Ekström et al. (2012), one finds the spectroscopic parameters of Fitzpatrick & Massa (2005) for $\kappa$ And A consistent with ages of ∼220 Myr and ∼200 Myr, respectively. We conclude that the combination of $T_{\rm eff}$ and log($g$) for $\kappa$ And are consistent with an isochronal age of ∼200 Myr, however it may be as old as ∼300 Myr if the star is indeed metal poor. As we show in the next section, these age estimates are commensurate with that inferred through comparison of the HR diagram position to evolutionary tracks.

#### 3.2.3. *Luminosity vs. $T_{\rm eff}$ Analysis*

In Figure 10, we plot the HR diagram position for $\kappa$ And (adopting the $T_{\rm eff}$ from Fitzpatrick & Massa (2005), with the revised luminosity from § 3.1 along with evolutionary tracks and isochrones from Bertelli et al. (2009) assuming approximately protosolar composition (Y = 0.27, Z = 0.017). Sampling within the $T_{\rm eff}$and luminosity uncertainties using Gaussian deviates, we find that the HR diagram position is consistent with an age of $140 \pm 17$ Myr and mass $2.89 \pm 0.03$ $M_\odot$. Adopting the Bertelli et al. (2009) tracks for a slightly lower (yet plausible) helium mass fraction (Y = 0.26, Z = 0.017), the HR diagram point is consistent with age $139 \pm 17$ Myr ($2.90 \pm 0.03$ $M_\odot$). If we decrease the metal fraction by

$\Delta Z = 0.001$ (Y = 0.27, Z = 0.016), this shifts the age slightly older: $152 \pm 16$ Myr ($2.84 \pm 0.03\ M_\odot$). Lowering the metal fraction to levels suggested for the proto-Sun informed by recent observations using 3D solar atmosphere models (e.g. Asplund et al. 2009) (Y = 0.27, Z = 0.014), one would derive $177 \pm 15$ Myr ($2.79 \pm 0.03\ M_\odot$). We can also estimate an isochronal age which assumes that the measured photospheric metallicity is indicative of the star's bulk composition ([Fe/H∼-0.36]). We scale the star's chemical composition by assuming a linear trend in $\Delta Y/\Delta Z = 1.57$, which connects the Big Bang primordial abundances (Y = 0.248, Z = 0.00; Steigman 2010) with the solar photospheric ratio (X/Z) and protosolar Y estimated by (Asplund et al. 2009). Adopting the metallicity from Fitzpatrick & Massa (2005) ([Fe/H] = -0.36), we interpolate an approximate chemical composition of Y = 0.26, Z = 0.006. Using this subsolar chemical composition, we infer that the HR diagram position of $\kappa$ And would be consistent with age $317 \pm 10$ Myr and mass $2.52 \pm 0.03\ M_\odot$. Note that this chemical composition represents almost certainly a strong lower limit to the plausible helium and metal mass fractions, and hence defines an upper limit on the star's age and a lower limit on its mass.

As a check, we evalulate the HR diagram position of $\kappa$ And A using other sets of tracks. Using the Girardi et al. (2000) evolutionary tracks for [Fe/H] = $0.0 \pm 0.1$ via the online isochrone interpolator PARAM 1.1[20], we find that $\kappa$ And's HR diagram position[21] corresponds to age $252 \pm 33$ Myr and mass $2.60 \pm 0.06\ M_\odot$, with surface gravity $\log(g) = 4.12 \pm 0.02$. Assuming [Fe/H] = 0, the same tracks yield an age of 121 Myr, mass of 2.85 $M_\odot$ and $\log(g) = 4.17$. Using the rotating evolutionary tracks from Georgy et al. (2013) for their assumed solar composition (Z = 0.014) and $v_{rot}/v_{crit} = 0.3$, $\kappa$ And's age is approximately 250 Myr for mass 2.75 $M_\odot$. Combining our estimate of the mass of $\kappa$ And A (∼2.8 $M_\odot$) with our updated radius estimate in Table 2 (2.29 $R_\odot$) leads to an estimate of the star's critical rotational velocity of ∼480 km s$^{-1}$, hence for $v\sin i$ = 150 km s$^{-1}$(Abt et al. 2002), $v_{eq}/v_{crit} > 0.3$. Hence, the evolutionary tracks that include rotation which show slightly older (∼10%) ages, are probably to be favored.

If the star's bulk composition is similar to solar (Z ≃ 0.015-0.017), the age is likely to be $\sim 180 \pm 70$ Myr. If the star's bulk composition reflects its photospheric abundances (Z ≃ 0.006), then the star may be of order $\sim 250 \pm 70$ Myr. Hence, there is a systematic uncertainty in the age at the ∼40% level due to the uncertainty in the bulk metal fraction of the star. Uncertainties due to the helium fraction, observational uncertainties, rotation, and other differences between the input physics of the different stellar evolutionary models, each contribute to the age uncertainty at the ∼10% level. *We conclude that the HR diagram position for the star is consistent with an approximate age of $220 \pm 100$ Myr and mass $2.8^{+0.1}_{-0.2}\ M_\odot$.* The derived isochronal age range from the HR diagram analysis is commensurate with that from the $T_{\rm eff}$ vs. $\log(g)$ analysis in §3.2.2.

[20] http://stev.oapd.inaf.it/cgi-bin/param_1.1

[21] Instead of inputting luminosity directly, we entered the V magnitude and parallax listed in Table 2, along with the Fitzpatrick & Massa (2005) $T_{\rm eff}$ and metallicity.

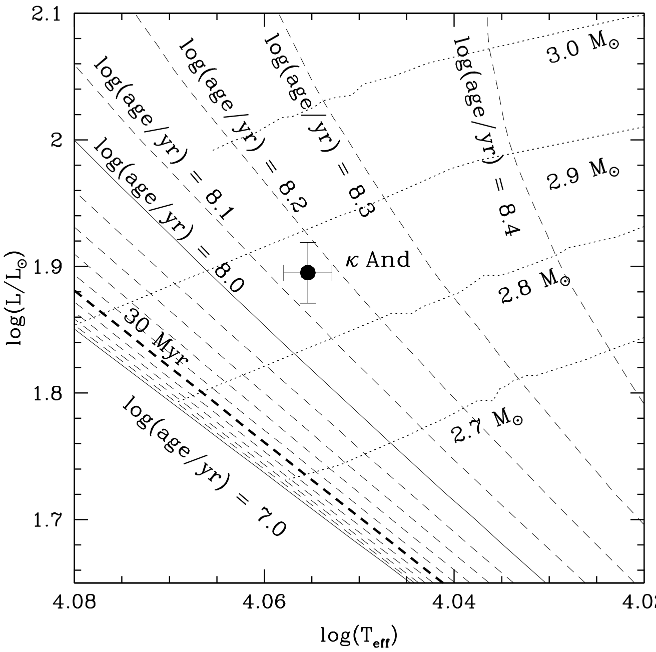


Fig. 10.— Theoretical HR diagram position for $\kappa$ And with Bertelli et al. (2009) evolutionary tracks for solar composition (Y = 0.27, Z = 0.017) overlain. The 30 Myr isochrone (log(age/yr) =7.5) is shown as a thick dashed line. Using these tracks, $\kappa$ And has age 140 Myr. Tracks which include rotation and lower metallicity produce systematically older ages. Taking into account uncertainties in the composition (assuming the star has bulk composition ranging from [Fe/H]=-0.36 to solar), we estimate an isochronal age of $220 \pm 100$ Myr.

Our new estimate of $220 \pm 100$ Myr is ∼7× older than the age estimate presented by Carson et al. (2013). Based on the combination of $T_{\rm eff}$, $\log(g)$, and luminosity, an age for $\kappa$ And A younger than 120 Myr or older than 320 Myr seem extremely unlikely. If the bulk composition of $\kappa$ And is truly as metal poor as the photosphere ([Fe/H] ≃ -0.3), then not only is $\kappa$ And ∼10× older than the 30 Myr-old Columba association, but its chemical composition contains less than half the metals of other Columba members.

With this revised age in hand, we use the DUSTY models of Chabrier et al. (2000) to estimate the mass of $\kappa$ And B. Using the $L$-band photometry from Bonnefoy et al. (2013b) with our revised age of 220±100 Myr, we find a revised mass of $50^{+16}_{-13}\ M_{Jup}$, where the uncertainty is driven almost entirely by our derived uncertainty in the age of $\kappa$ And A.

### 3.3. *Multiplicity*

High mass stars show a high degree of multiplicity (e.g. Duchêne & Kraus 2013, and references therein) and characterizing the multiplicity of the $\kappa$ And system, and hence the contributions to the observed system luminosity, has significant implications for its age (§3.2). An equal-flux binary companion would significantly bias the inferred luminosity (§3.1), lowering the $\log(L/L_\odot)$ value in Figure 10 by 0.3 dex, placing it near the 30 Myr age track. Hence, understanding the multiplicity of this system is crucial for a correct interpretation of Figure 10. Further, low-mass binary companions could be useful as additional age indicators. There have been numerous observations of $\kappa$ And with various techniques, but they have not been synthesized into a single set of limits. We therefore present new observations with nonredundant aperture-mask interferometry, as well as interpreting existing radial velocity and imaging data in the Appendix, and compile a comprehensive limit on the existence of binary companions at all semimajor axes (from $10^{-2}$ AU to $10^4$ AU).

#### 3.3.1. *New Limits from Nonredundant Mask Interferometry*

The technique of Aperture Masking Interferometry (sometimes referred to as "Sparse Aperture Masking" or "Non-Redundant Masking") is now well-established as a means of achieving the full diffraction limit of an AO-equipped telescope (Lloyd et al. 2006; Kraus et al. 2008; Lacour et al. 2011; Hinkley et al. 2011a, and references therein). We obtained new aperture masking observations of the $\kappa$ And system on 2012 December 2 UT, using Keck II and the facility adaptive optics imager (NIRC2). To maximize resolution and sensitivity to short-period binary companions, we used the $J_{cont}$ filter and an 18-hole aperture mask. For calibration, we also observed the stars HIP 114456 and HIP 116631.

$\kappa$ And was observed with two sets of 10 individual 10s integrations, and we observed each calibrator for one such observation. The data analysis follows the same prescription as in Kraus et al. (2008); Hinkley et al. (2011a); Kraus et al. (2011), so we refer the reader to these works. We summarize the detection limits as a function of projected separation in Table 4.

TABLE 4
Aperture Masking Interferometry Detection Limits

| Projected Sep (mas) | (AU) | $\Delta J$ (mag) | $M_{\rm sec}$ ($M_{Jup}$) |
|---|---|---|---|
| 10–20 | 0.5–1 | 4.23 | 70 |
| 20–40 | 1–2 | 5.55 | 32 |
| 40–80 | 2–4 | 5.46 | 34 |
| >80 | >4 | 5.42 | 35 |

Note. — Limiting companion masses are calculated for the null hypothesis that $\tau = 30$ Myr, since that is the hypothesis we are trying to disprove. The limiting masses for $\tau = 100$ Myr are still $<0.1\ M_\odot$ in all cases.

#### 3.3.2. *Limits on Stellar Binary Companions*

Utilizing the information on wide binary companions contained in the appendix, as well as archival radial velocities also listed in the appendix, we have combined all of the above data in a unified Monte Carlo simulation that computes detection rates as a function of companion mass and semimajor axis. We computed $10^3$ randomly generated orbits across a grid with bins of 0.1 $M_\odot$ in $M_{\rm secondary}$ (spanning 0.1–2.8 $M_\odot$) and 0.1 dex in $\log(a)$ (spanning $10^{-2}$ to 10 AU); we did not test wider separations because the aperture masking and Subaru coronagraphic observations published in Carson et al. (2013) rule out all stellar companions, and the radial velocity data is not useful for substellar companions. For each randomly generated orbit in the Monte Carlo, we tested the $\chi^2$ goodness of fit for the radial velocity time series while also verifying that the companion would not have been detected in any of the direct imaging epochs. We regarded a companion to be "ruled out" if the $\chi^2$ statistic is larger than the 95% confidence limit (i.e., the orbit would have produced a signal at >95% confidence). We present the resulting limits on stellar binary companions in Figure 11, which shows the percentage of stellar binary companions, as a function of companion mass and semimajor axis, that would have been detected by the radial velocity, aperture masking, and direct imaging observations. Nearly all stellar companions with $a \gtrsim 0.6-0.7$ AU are ruled out by the aperture masking observations, while radial velocities rule out the majority of short-period stellar companions with $M \gtrsim 0.5\ M_\odot$.

We note that there exists a region in which nearly equal mass (2-3 $M_\odot$) binary companions are not completely ruled out. However, in their work reporting observations with the Palomar Testbed Interferometer (PTI),

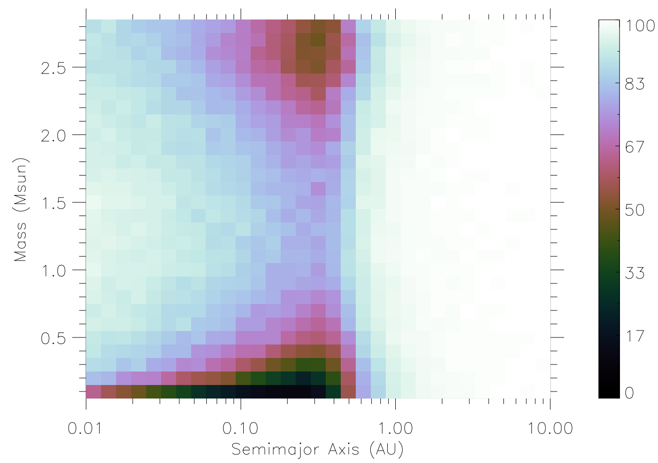


Fig. 11.— The percentage of stellar binary companions, as a function of companion mass and semimajor axis, that would have been detected by the radial velocity, aperture masking, and direct imaging observations that we summarize in Section 3.3 as well as this paper's appendix. The vertical color scale bar shows this percentage ranging from 0 to 100%. Nearly all stellar companions with $a \gtrsim 0.6-0.7$ AU are ruled out by the aperture masking observations, while radial velocities rule out the majority of short-period stellar companions with $M \gtrsim 0.5\ M_\odot$.

van Belle et al. (2008) did not find this system to be resolved. Further, given the resolution and field-of-view of PTI, this work should have reported a similar-brightness binary companion in their data. They claimed that even given the poor fit to a single point source, then the noise in the visibilities would have been consistent with a companion showing 4 magnitudes of K-band contrast or more, rather than 0 or 1 magnitudes of contrast. Thus, we can appeal to their results to argue that nothing lies in the regime which is not formally ruled out by our analysis.

Our analysis suggests that the luminosity of the $\kappa$ And system is not biased in any meaningful way by binarity of any kind, and that the calculated luminosity plotted in Figure 10 is due solely to a single host star: $\kappa$ And A, reinforcing our isochronal $220 \pm 100$ Myr age estimate.

### 3.4. *Constraints on Inclination*

In this section we investigate the likelihood that $\kappa$ And A is a nearly pole-on fast-rotator. Such a configuration could account for the position of $\kappa$ And in the HR diagram (Figure 10), while still possessing the previously reported age of 30 Myr. While effects induced by rapid rotation and inclined viewing angles can lead to scatter in diagrams such as Figure 9 and color-magnitude diagrams, thereby confusing the age analysis, such effects are less important for $\kappa$ And as we show below. Specifically, an extreme pole-on orientation is not possible for $\kappa$ And due to its high observed rotational velocity. However, even very low-inclination models would not change the modelled age noticeably: these models cause the star to become not just more luminous, but also hotter. Thus, on an HR diagram, the effect of rotation and inclination is mostly to shift the star along, and not across, an isochrone.

Nonetheless, the observed properties of $\kappa$ And allow us to place some constraints on its inclination. With a projected rotational velocity is $v\sin i = 150$ km/s (Abt et al. 2002), and taking the approximate mass and radius of $\kappa$ And listed in Table 3, the formulae of Townsend et al. (2004) predict that the critical rotational velocity for $\kappa$ And to be 394 km/s, which is indeed typical for B9 stars (Table 1 of Townsend et al. 2004). Since we do not know the ratio of the star's equatorial to polar radii, we have adopted the radius inferred from the luminosity and effective temperature as the star's polar radius in the formula presented in Townsend et al. (2004). A lower limit to the ratio of the aspect ratio $r_{eq}/r_{polar}$ can be estimated via the Roche approximation formula from Townsend et al. (2004), where $v\sin i = 150$ km/s places a lower limit on the equatorial velocity of the star. We estimate $r_{eq}/r_{polar} > 1.05$. The combination of $v\sin i$ and predicted critical velocity lead to a constraint on the inclination of the star: $i > 22^\circ.4$. Hence the star can not be within 22° of pole-on in orientation.

As Townsend et al. (2004) demonstrate, a fast-rotating B star can get a boost in absolute magnitude and/or reddening in optical color due to the effects of gravity darkening and viewing angles. Fig. 3 of Townsend et al. (2004) is instructive for testing whether $\kappa$ And could be interpreted as a young, extremely fast rotator seen at high inclination. In Figure 3 of Townsend et al. (2004), the authors take non-rotating B-type stars (conveniently including a fiducial B9 dwarf) and calculate the effects of gravity darkening and viewing angle on $B-V$ color and absolute V magnitude for a range of rotation velocities (ranging from non-rotating to near critical $v_{eq}/v_{crit}$ = 0.95) and at three different inclination angles (0°, 45°, 90°). As discussed previously, the $v\sin i$ constraints are consistent with $v_{eq}/v_{crit} > 0.38$ and $i > 22^\circ$. So we can already rule out $\kappa$ And being a near face-on star rotating near $v_{crit}$. For Townsend et al.'s models, it is the face-on orientation ($i = 0^\circ$) that produces the greatest brightening in absolute magnitude, approximately ∼0.6 magnitude in $M_V$ for their most optimistic model ($i = 0^\circ$, $v_{eq}/v_{crit} = 0.95$). The absolute magnitude of $\kappa$ And is similar to that of late B-type Pleiades (∼120 Myr), and approximately ∼0.4 mag brighter than the ZAMS of Schmidt-Kaler (1982), which is a reasonable approximation for the sequence of ∼30 Myr late B-type stars. While the $i = 45^\circ$ and 90° models of Townsend et al. (2004) are plausible for $\kappa$ And, the $i = 0^\circ$ is not. Interpolating amongst the predicted differences in absolute magnitude and color for the fiducial B9 model of Townsend et al. (2004), it appears that it is extremely difficult to get a plausible model that can provide a ∼0.4 mag boost in absolute magnitude. For $i \simeq 22$ (roughly halfway between the $i = 0^\circ$ and 45° models), $\kappa$ And would have to be rotating at or near critical velocity i.e. $v_{eq}/v_{crit} \simeq 0.95$. More modest inclinations of $i = 45^\circ$ and 90° can not provide sufficient brightening of the star's real absolute magnitude to the observed value.

Measurement of a photometric rotation period for the star could provide a measure of the star's rotation, as well as interferometric diameter measurements to test whether the star is consistent with an extreme aspect ratio. While included as a suspected variable star in the GCVS catalog (Samus et al. 2007), the Hipparcos survey found the star to be remarkably photometrically quiet (classified "C" = constant), with scatter in Hp magnitudes of only 0.004 mag, hence measuring a photometric period may be challenging.

### 3.5. *Kinematics*

Given the evidence presented that the $\kappa$ And system is $\gtrsim$220 Myr, it is worthwhile to revisit the original Zuckerman et al. (2011a) assignment of this system to the 30 Myr Columba Association. Using the position, proper motion, and parallax from van Leeuwen (2007) and mean radial velocity from Gontcharov (2006), we estimate the velocity of $\kappa$ And to be ($U$, $V$, $W$) = (-11.5 $\pm$ 0.3, -20.1 $\pm$ 0.5, -5.9 $\pm$ 0.6 ) and ($X$, $Y$, $Z$)= (-16.7, 46.5, -14.8). As noted in Carson et al. (2013), the space velocity and position of $\kappa$ And yield >95% probability of Columba membership according to the moving group prediction method (Malo et al. 2013). However, *this 95% probability was only for an additional hypothesis in which a 0.75 magnitude shift was applied to the photometric sequence for the association to account for possible unresolved binarity, a case which we rule out in §3.3.* The probability for a non-binary case carries a lower probability, although this value was not tabulated in Malo et al. (2013). Additionally, further investigation reveals that $\kappa$ And was included as a bona fide member of the collection of stars comprising the Columba group kinematics in this work. This fact automatically increases its derived probability for membership in Columba.

Figure 12 shows the UVWXYZ velocities and positions for the 21 bona fide Columba members listed in Malo et al. (2013) with the $\kappa$ And system highlighted. Figure 12 shows that the $UVW$ velocities for $\kappa$ And are consistent with the 20 other bona fide members of Columba. However it is a 2.7$\sigma$ outlier in galactic Y position, having the largest Y position of the entire Columba ensemble. Even further, Zuckerman et al. (2011a) do not use the galactic Y position as part of their criteria for moving group membership.

The strong agreement between the $UVW$ velocity of $\kappa$ And B and the Columba association make a full kinematic "traceback" analysis challenging. Despite the fact that this object is a significant positional outlier in the $Y$-direction, any discussion on the star's past position, velocity relative to the centroid of the Columba association, etc. is weakened due to the similarities in velocities of the star and the Columba group discussed above. Further, the errors in velocities for $\kappa$ And A and Columba are sizeable (∼0.5 km/s and ∼1 km/s, respectively). Nonetheless, adopting the centroid position and $UVW$ velocity for Columba listed in Malo et al. (2013) , and the $UVW$ for $\kappa$ And A listed in Table 1, the star is currently 80

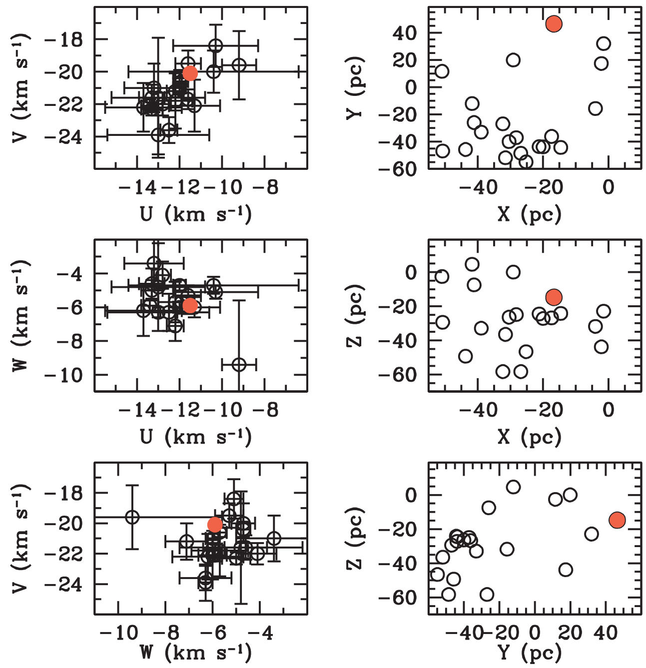


FIG. 12.— The UVWXYZ velocities and positions for the 20 bona fide Columba members (open circles) listed in Malo et al. (2013) while the filled (orange) symbol indicates the $\kappa$ And system. While the UVW values for $\kappa$ And are in agreement with those for the Columba group, it has the largest Y position of the group.

pc away from the centroid of Columba, and its velocity differs by  1.5 km/s. Using an epicycle orbit approximation code, it appears that $\kappa$ And was only slightly closer to the Columba centroid in the past:  18 Myr ago it was 60 pc from Columba, and  30 Myr ago it was  74 pc from Columba.

However, the outlying $Y$ position of $\kappa$ And (46.5pc) raises questions about the likelihood of its formation near the Columba groups centroid ($Y$=-31.3). Notably, for $\kappa$ And to have formed near Columba's centroid 30 Myr ago, it would have had to inherited a peculiar V velocity of $\Delta V$ = (46.5 + 31.3pc)/(30 Myr) = 2.59 pc/Myr $\sim$ 2.6 km/s. Given Columba's current $V$ velocity of $V$=-21.3, a "runaway" star would have velocity $V + \Delta V \simeq$ -18.7 km/s. However, this is still within $\sim 1\sigma$ of what is observed for $\kappa$ And.

## 4. SUMMARY

In this work we have presented analysis of the spectra and photometry of the companion $\kappa$ And B, as well as presented a comprehensive analysis of the age, multiplicity, and moving group kinematics of the $\kappa$ And AB system. We summarize our results as follows:

- $YJH$-band low resolution spectra obtained through high contrast imaging with Project 1640 are consistent with an intermediate age ($\lesssim$300 Myr) brown dwarf with L1$\pm$1 spectral type, although similiarities with field mid-L objects are present.

- By fitting synthetic models to the Project 1640 spectrophotometry, we constrain the surface gravity and effective temperature of $\kappa$ And B to be log($g$)=$4.33^{+0.88}_{-0.79}$ and $T_{\rm eff}$=2040K$^{+58}_{-64}$, respectively.

- Comparing these photospheric properties to theoretical isochrones in log($g$) and $T_{\rm eff}$ parameter space indicates an age much older than the 30 Myr age reported previously for $\kappa$ And B.

- Previously published log($g$) and $T_{\rm eff}$ values for $\kappa$ And A are compared to theoretical isochrones, indicating ages of $\sim$100-300 Myr. The HR diagram position of $\kappa$ And A is consistent with the same age for a range of assumed chemical compositions. Taken together, the stellar parameters are consistent with an isochronal age of $220 \pm 100$ Myr, where the age uncertainty is dominated by the star's chemical composition.

- We combine aperture masking interferometry, archival radial velocity data from the literature, and archival multi-epoch imaging of $\kappa$ And A to rule out any faint stellar companions beyond $\sim$0.6 AU (Figures 11 and 13) that could be causing the star to be overluminous for the originally-quoted 30 Myr age. In addition, we show that a nearly "pole-on" viewing angle coupled with extremely rapid rotation is unlikely to be the configuration contributing to this star's overluminosity.

- $\kappa$ And A appears to be a kinematic outlier compared to other Columba members. While the velocity of $\kappa$ And is consistent with that of other Columba members, its Galactic Y position is an outlier. Taken together with its overluminosity and low surface gravity expected for a 30 Myr old, late-B star, $\kappa$ And is most likely an interloper to the Columba association.

- Through the use of Hertzsprung-Russell diagram analysis as well as comparison of the log($g$) and $T_{\rm eff}$ parameters for $\kappa$ And A with theoretical isochrones, we have shown that the star has an age closer to 220 Myr than the originally assumed 30 Myr based on association with Columba. These ages indicate that the mass of $\kappa$ And B is $50^{+16}_{-13}$ $M_{Jup}$, rather than the previously claimed 12-14 Jupiter Masses.

We thank the anonymous referee for numerous helpful suggestions. SH is supported by an NSF Astronomy and Astrophysics Postdoctoral Fellowship under award AST-1203023. LP performed this work in part under contract with the California Institute of Technology funded by NASA through the Sagan Fellowship Program. ALK was supported by a Clay Fellowship. EEM is supported by NSF award AST-1008908 and generous donations of Gabriela Mistral Pisco. GV is supported by a NASA OSS grant NMO7110830/ 102190. RN performed this work with funding through a grant from Helge Axson Johnson's foundation. JRC is supported by NASA Origins of Solar Systems Grant NNX13AB03G. A portion of this work is or was supported by the National Science Foundation under Grant Numbers AST-0215793, 0334916, 0520822, 0804417 and 1245018. A portion of the research in this paper was carried out at the Jet Propulsion Laboratory, California Institute of Technology, under a contract with the National Aeronautics and

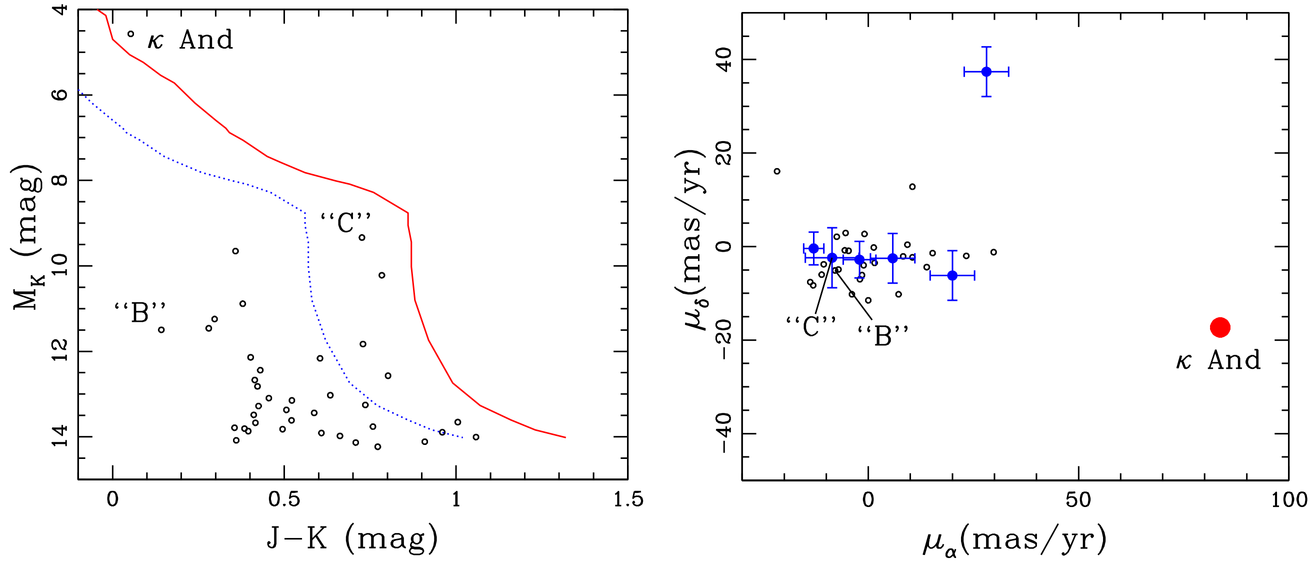


FIG. 13.— Left: A 2MASS ($M_K$,$J-K$) color-magnitude diagram for the 38 sources with $K < 14.3$ that are located within $\rho$ =20–300″ of $\kappa$ And. The solid red line is the main sequence at the distance of $\kappa$ And (Kraus & Hillenbrand 2007), while the blue dotted line shows the $\Delta(J-K) < 0.3$ limit which denotes possible consistency. Only seven sources (including "C", but excluding "B") have colors which are marginally consistent with physical association. Right: A proper-motion diagram for the 34 sources which have catalog proper motions. The blue points denote 6 of the 7 sources with marginally consistent colors. None of these sources (including both "B" and "C") are comoving with $\kappa$ And. Visual inspection of the original POSS-I red plate (epoch 1952) and the 2MASS $K$ band image (epoch 1998) show that the remaining four sources have proper motions of <20 mas/yr, and hence also are not comoving. We therefore conclude that the purported "B" and "C" components are not physically associated, and neither are any other sources with $M_{lim} > 15$ $M_{Jup}$ (if $\tau = 30$ Myr) and $\rho$ =1000-15000 AU.

Space Administration and was funded by internal Research and Technology Development funds. Our team is also grateful to the Plymouth Hill Foundation, and an anonymous donor, as well as the efforts of Mike Werner, Paul Goldsmith and Jacob van Zyl. Any opinions, findings, and conclusions or recommendations expressed in this material are those of the authors and do not necessarily reflect the views of the National Science Foundation. Finally, the entire team expresses is sincere gratitude and appreciation for the hard work of the Palomar mountain crew, especially by Steve Kunsman, Mike Doyle, Greg van Idsinga, Bruce Baker, Jean Mueller, Kajsa Peffer, Kevin Rykowski, Carolyn Heffner and Dan McKenna. This project would be impossible without the flexibility, responsiveness and dedication of such an effective and motivated staff.

## APPENDIX

## LIMITS ON WIDE COMPANIONS TO $\kappa$ AND

Here we present limits on wide binary companions to the $\kappa$ And system as well as a listing of archival radial velocities. These results are incorporated into our analysis presented in §3.3.

### *Literature Observations*

The primary star $\kappa$ And A has been observed by numerous radial velocity surveys over the past century; we list those radial velocity observations which we could recover in Table 5. Palmer et al. (1968) reported 11 radial velocity measurements for $\kappa$ And that were taken between 1960 October 4 and 1961 November 4 (UT), and found a mean radial velocity of $v = -15$ km/s with a standard deviation of $\sigma = 10.5$ km/s and a standard deviation of the mean of $\sigma_\mu = 3$ km/s. Harper (1937) reported 3 radial velocity measurements that were taken between 1923 Sep 13 and 1926 Dec 14 (UT), and found a mean radial velocity of $v = -19$ km/s with a standard deviation of $\sigma = 5$ km/s and a standard deviation of the mean of $\sigma_\mu = 3$ km/s; since there are only three epochs and we must be concerned with zero point shifts, we do not use these data. Wilson (1953) reported that $\kappa$ And had a mean radial velocity of $v = -9.0$ km/s for 10 observations, but did not report an uncertainty or the individual measurements, so we cannot use these measurements either. Finally, we also note that Huang & Gies (2008) reported that $\kappa$ And is a relatively fast rotator ($v_{rot} = 169$ km/s), and therefore even if it is a low-amplitude double-lined spectroscopic binary, radial velocity measurements might not resolve the individual components. Our analysis therefore must consider the shift in spectral line centroids in placing constraints on the presence of a double-lined spectroscopic binary.

### *Limits on Wide Co-moving Companions with Archival Multi-Epoch Imaging*

Even before the discovery of $\kappa$ And "b", $\kappa$ And was considered a binary (ADS 16916, WDS 23404+4420, HJ 1898). J.F.W. Herschel reported (Herschel 1831) possible companions to $\kappa$ And at $\rho = 35''$ ("B") in epoch 1828 and $\rho = 98''$

TABLE 5
Radial Velocities

| Epoch (JD) | $v$ (km/s) | $\sigma_v$ (km/s) | Source |
|---|---|---|---|
| 2437212.34 | -9 | 7 | Palmer et al. (1968) |
| 2437215.41 | -14 | 3 | Palmer et al. (1968) |
| 2437222.44 | -14 | 5 | Palmer et al. (1968) |
| 2437223.36 | +9 | 9 | Palmer et al. (1968) |
| 2437230.50 | -9 | 8 | Palmer et al. (1968) |
| 2437243.45 | -29 | 10 | Palmer et al. (1968) |
| 2437558.50 | -25 | 4 | Palmer et al. (1968) |
| 2437587.41 | -4 | 8 | Palmer et al. (1968) |
| 2437590.46 | -21 | 3 | Palmer et al. (1968) |
| 2437601.52 | -17 | 5 | Palmer et al. (1968) |
| 2437608.38 | -18 | 7 | Palmer et al. (1968) |
| 2423676.791 | -19.4 | ... | Harper (1937) |
| 2423676.818 | -13.4 | ... | Harper (1937) |
| 2424963.659 | -24.2 | ... | Harper (1937) |

("C") in epoch 1836 (Smyth 1844; Mason et al. 2001). The nearest 2MASS counterparts for these stars are 2MASS J23402285+4419177 ($\rho = 48''$) and 2MASS J23401480+4420469 ($\rho = 113''$). If these (or any other) stars were indeed associated, then they would offer a valuable check on the age of the system. To test the association of these candidates and to search for other potential comoving companions, we have investigated the nature of all identifiable sources within $<5'$ (<15000 AU) of $\kappa$ And.

We queried the 2MASS Point Source Catalog (which has the highest image fidelity) to identify 38 candidate companions with $K < 14.3$ and $\rho < 5'$. The PSC clearly detected a source with $K = 13.9$ at $\rho = 27''$, and the background flux is similar down to $\rho = 20''$. We therefore estimate that any source brighter than the 2MASS detection limit ($K = 14.3$ at $10\sigma$) would have been detected at $\rho > 20''$. We also compiled proper motions for most of these sources from UCAC4 (for 9 sources; Zacharias et al. 2012) and from PPMXL (for 25; Roeser et al. 2010). Four candidate companions did not have proper motions in either catalog, but in all cases, visual inspection of the raw images showed that they moved by $<1''$ ($\lesssim$20 mas/yr) between the POSS-I epoch (1952) and the 2MASS epoch (1998).

In Figure 13 (left), we show a $(J-K, K)$ color-magnitude diagram for the 38 sources with $K < 14.3$ identified by 2MASS. Figure 13 also shows the main sequence for stars located at the distance of $\kappa$ And. Only 7 sources are located within $\Delta(J-K) < 0.3$ mag of the main sequence; the remaining 31 sources (including the "B" companion from 1831, as well as three of the four sources with visually-estimated proper motions) appear to be unassociated background stars. In Figure 13 (right), we show a proper motion diagram for the 34 sources with measured proper motions. None agree with the HIPPARCOS proper motion for $\kappa$ And to within $3\sigma$ (including both "B" and "C" objects from 1831), and hence all (including the fourth star with a visually estimated proper motion limit) appear to be unassociated background sources. We therefore conclude that there are no comoving companions (including the purported "B" and "C" companions) with $K < 14.3$ ($M_{lim} > 15\ M_{Jup}$, for the null hypothesis of $\tau = 30$ Myr) located within $\rho =$20–300$''$ ($\rho =$ 1000–15000 AU) of $\kappa$ And.

## REFERENCES


Absil, O., & Mawet, D. 2010, A&A Rev., 18, 317
Abt, H. A., Levato, H., & Grosso, M. 2002, ApJ, 573, 359
Allard, F., Hauschildt, P. H., Alexander, D. R., Tamanai, A., & Schweitzer, A. 2001, ApJ, 556, 357
Allende Prieto, C., & Lambert, D. L. 1999, A&A, 352, 555
Allers, K. N., & Liu, M. C. 2013, ApJ, 772, 79
Asplund, M., Grevesse, N., Sauval, A. J., & Scott, P. 2009, ARA&A, 47, 481
Baraffe, I., Chabrier, G., Allard, F., & Hauschildt, P. H. 2002, A&A, 382, 563
Barman, T. S., Hauschildt, P. H., & Allard, F. 2001, ApJ, 556, 885
Bertelli, G., Nasi, E., Girardi, L., & Marigo, P. 2009, A&A, 508, 355
Bonnefoy, M., Chauvin, G., Lagrange, A.-M., Rojo, P., Allard, F., Pinte, C., Dumas, C., & Homeier, D. 2013a, ArXiv e-prints
Bonnefoy, M., Currie, T., Marleau, G.-D., Schlieder, J. E., Wisniewski, J., Carson, J., Covey, K. R., Henning, T., Biller, B., Hinz, P., Klahr, H., Marsh Boyer, A. N., Zimmerman, N., Janson, M., McElwain, M., Mordasini, C., Skemer, A., Bailey, V., Defrère, D., Thalmann, C., Skrutskie, M., Allard, F., Homeier, D., Tamura, M., Feldt, M., Cumming, A., Grady, C., Brandner, W., Kandori, R., Kuzuhara, M., Fukagawa, M., Kwon, J., Kudo, T., Hashimoto, J., Kusakabe, N., Abe, L., Brandt, T., Egner, S., Guyon, O., Hayano, Y., Hayashi, M., Hayashi, S., Hodapp, K., Ishii, M., Iye, M., Knapp, G., Matsuo, T., Mede, K., Miyama, M., Morino, J.-I., Moro-Martin, A., Nishimura, T., Pyo, T., Serabyn, E., Suenaga, T., Suto, H., Suzuki, R., Takahashi, Takami, M., Takato, N., Terada, H., Tomono, D., Turner, E., Watanabe, M., Yamada, T., Takami, H., & Usuda, T. 2013b, ArXiv e-prints
Bowler, B. P., Liu, M. C., Shkolnik, E. L., & Dupuy, T. J. 2013, ApJ, 774, 55
Bressan, A., Marigo, P., Girardi, L., Salasnich, B., Dal Cero, C., Rubele, S., & Nanni, A. 2012, MNRAS, 427, 127
Burgasser, A. J., Liu, M. C., Ireland, M. J., Cruz, K. L., & Dupuy, T. J. 2008, ApJ, 681, 579

Carson, J., Thalmann, C., Janson, M., Kozakis, T., Bonnefoy, M., Biller, B., Schlieder, J., Currie, T., McElwain, M., Goto, M., Henning, T., Brandner, W., Feldt, M., Kandori, R., Kuzuhara, M., Stevens, L., Wong, P., Gainey, K., Fukagawa, M., Kuwada, Y., Brandt, T., Kwon, J., Abe, L., Egner, S., Grady, C., Guyon, O., Hashimoto, J., Hayano, Y., Hayashi, M., Hayashi, S., Hodapp, K., Ishii, M., Iye, M., Knapp, G., Kudo, T., Kusakabe, N., Matsuo, T., Miyama, S., Morino, J., Moro-Martin, A., Nishimura, T., Pyo, T., Serabyn, E., Suto, H., Suzuki, R., Takami, M., Takato, N., Terada, H., Tomono, D., Turner, E., Watanabe, M., Wisniewski, J., Yamada, T., Takami, H., Usuda, T., & Tamura, M. 2013, ApJ, 763, L32
Chabrier, G., Baraffe, I., Allard, F., & Hauschildt, P. 2000, ApJ, 542, 464
Chauvin, G., Lagrange, A., Dumas, C., Zuckerman, B., Mouillet, D., Song, I., Beuzit, J., & Lowrance, P. 2004, A&A, 425, L29
Chauvin, G., Lagrange, A.-M., Zuckerman, B., Dumas, C., Mouillet, D., Song, I., Beuzit, J.-L., Lowrance, P., & Bessell, M. S. 2005, A&A, 438, L29
Chen, L., Hou, J. L., & Wang, J. J. 2003, AJ, 125, 1397
Cowley, A., Cowley, C., Jaschek, M., & Jaschek, C. 1969, AJ, 74, 375
Crepp, J. R., Pueyo, L., Brenner, D., Oppenheimer, B. R., Zimmerman, N., Hinkley, S., Parry, I., King, D., Vasisht, G., Beichman, C., Hillenbrand, L., Dekany, R., Shao, M., Burruss, R., Roberts, L. C., Bouchez, A., Roberts, J., & Soummer, R. 2011, ApJ, 729, 132
Cucchiaro, A., Macau-Hercot, D., Jaschek, M., & Jaschek, C. 1977, A&AS, 30, 71
Dekany, R. G., Brack, G., Palmer, D., Oppenheimer, B. R., Hayward, T. L., & Brandl, B. 1998, in Presented at the Society of Photo-Optical Instrumentation Engineers (SPIE) Conference, Vol. 3353, Proc. SPIE Vol. 3353, p. 56-59, Adaptive Optical System Technologies, Domenico Bonaccini; Robert K. Tyson; Eds., ed. D. Bonaccini & R. K. Tyson, 56–59
Digby, A. P., Hinkley, S., Oppenheimer, B. R., Sivaramakrishnan, A., Lloyd, J. P., Perrin, M. D., Roberts, Jr., L. C., Soummer, R., Brenner, D., Makidon, R. B., Shara, M., Kuhn, J., Graham, J., Kalas, P., & Newburgh, L. 2006, ApJ, 650, 484
Duchêne, G., & Kraus, A. 2013, ArXiv e-prints
Dupuy, T. J., & Liu, M. C. 2012, ApJS, 201, 19
Ekström, S., Georgy, C., Eggenberger, P., Meynet, G., Mowlavi, N., Wyttenbach, A., Granada, A., Decressin, T., Hirschi, R., Frischknecht, U., Charbonnel, C., & Maeder, A. 2012, A&A, 537, A146
Faherty, J. K., Burgasser, A. J., Walter, F. M., Van der Bliek, N., Shara, M. M., Cruz, K. L., West, A. A., Vrba, F. J., & Anglada-Escudé, G. 2012, ApJ, 752, 56
Faherty, J. K., Rice, E. L., Cruz, K. L., Mamajek, E. E., & Núñez, A. 2013, AJ, 145, 2
Fitzpatrick, E. L., & Massa, D. 2005, AJ, 129, 1642
Garrison, R. F., & Gray, R. O. 1994, AJ, 107, 1556
Georgy, C., Ekström, S., Granada, A., Meynet, G., Mowlavi, N., Eggenberger, P., & Maeder, A. 2013, ArXiv e-prints
Girardi, L., Bressan, A., Bertelli, G., & Chiosi, C. 2000, A&AS, 141, 371
Gontcharov, G. A. 2006, Astronomy Letters, 32, 759
Grosbol, P. J. 1978, A&AS, 32, 409
Harper, W. E. 1937, Publications of the Dominion Astrophysical Observatory Victoria, 7, 1
Hauschildt, P. H., Baron, E., & Allard, F. 1997, ApJ, 483, 390
Herschel, J. F. W. 1831, Memoirs of the Royal Astronomical Society, 4
Hill, G. M. 1995, A&A, 294, 536
Hinkley, S., Carpenter, J. M., Ireland, M. J., & Kraus, A. L. 2011a, ApJ, 730, L21+
Hinkley, S., Hillenbrand, L., Oppenheimer, B. R., Rice, E. L., Pueyo, L., Vasisht, G., Zimmerman, N., Kraus, A. L., Ireland, M. J., Brenner, D., Beichman, C., Dekany, R., Roberts, J. E., Parry, I. R., Roberts, Jr., L. C., Crepp, J. R., Burruss, R., Wallace, J. K., Cady, E., Zhai, C., Shao, M., Lockhart, T., Soummer, R., & Sivaramakrishnan, A. 2013, ApJ, 763, L9
Hinkley, S., Monnier, J. D., Oppenheimer, B. R., Roberts, L. C., Ireland, M., Zimmerman, N., Brenner, D., Parry, I. R., Martinache, F., Lai, O., Soummer, R., Sivaramakrishnan, A., Beichman, C., Hillenbrand, L., Zhao, M., Lloyd, J. P., Bernat, D., Vasisht, G., Crepp, J. R., Pueyo, L., Shao, M., Perrin, M. D., King, D. L., Bouchez, A., Roberts, J. E., Dekany, R., & Burruss, R. 2011b, ApJ, 726, 104
Hinkley, S., Oppenheimer, B. R., Brenner, D., Parry, I. R., Sivaramakrishnan, A., Soummer, R., & King, D. 2008, in Society of Photo-Optical Instrumentation Engineers (SPIE) Conference Series, Vol. 7015, Society of Photo-Optical Instrumentation Engineers (SPIE) Conference Series, pp. 701519–701519–10
Hinkley, S., Oppenheimer, B. R., Brenner, D., Zimmerman, N., Roberts, L. C., Parry, I. R., Soummer, R., Sivaramakrishnan, A., Simon, M., Perrin, M. D., King, D. L., Lloyd, J. P., Bouchez, A., Roberts, J. E., Dekany, R., Beichman, C., Hillenbrand, L., Burruss, R., Shao, M., & Vasisht, G. 2010, ApJ, 712, 421
Hinkley, S., Oppenheimer, B. R., Soummer, R., Sivaramakrishnan, A., Roberts, Jr., L. C., Kuhn, J., Makidon, R. B., Perrin, M. D., Lloyd, J. P., Kratter, K., & Brenner, D. 2007, ApJ, 654, 633
Hinkley, S., Oppenheimer, B. R., Zimmerman, N., Brenner, D., Parry, I. R., Crepp, J. R., Vasisht, G., Ligon, E., King, D., Soummer, R., Sivaramakrishnan, A., Beichman, C., Shao, M., Roberts, L. C., Bouchez, A., Dekany, R., Pueyo, L., Roberts, J. E., Lockhart, T., Zhai, C., Shelton, C., & Burruss, R. 2011c, PASP, 123, 74
Huang, W., & Gies, D. R. 2008, ApJ, 683, 1045
Ireland, M. J., Kraus, A., Martinache, F., Law, N., & Hillenbrand, L. A. 2011, ApJ, 726, 113
Katz, D., Soubiran, C., Cayrel, R., Barbuy, B., Friel, E., Bienaymé, O., & Perrin, M.-N. 2011, A&A, 525, A90
Kirkpatrick, J. D. 2005, ARA&A, 43, 195
Kirkpatrick, J. D., Looper, D. L., Burgasser, A. J., Schurr, S. D., Cutri, R. M., Cushing, M. C., Cruz, K. L., Sweet, A. C., Knapp, G. R., Barman, T. S., Bochanski, J. J., Roellig, T. L., McLean, I. S., McGovern, M. R., & Rice, E. L. 2010, ApJS, 190, 100
Kraft, R. P. 1967, ApJ, 150, 551
Kraus, A. L., & Hillenbrand, L. A. 2007, ApJ, 662, 413
Kraus, A. L., Ireland, M. J., Hillenbrand, L. A., & Martinache, F. 2011, ArXiv e-prints
Kraus, A. L., Ireland, M. J., Martinache, F., & Lloyd, J. P. 2008, ApJ, 679, 762
Lacour, S., Tuthill, P., Amico, P., Ireland, M., Ehrenreich, D., Huelamo, N., & Lagrange, A.-M. 2011, A&A, 532, A72
Lafrenière, D., Jayawardhana, R., & van Kerkwijk, M. H. 2008, ApJ, 689, L153
Lafrenière, D., Marois, C., Doyon, R., Nadeau, D., & Artigau, É. 2007, ApJ, 660, 770
Leconte, J., Soummer, R., Hinkley, S., Oppenheimer, B. R., Sivaramakrishnan, A., Brenner, D., Kuhn, J., Lloyd, J. P., Perrin, M. D., Makidon, R., Roberts, Jr., L. C., Graham, J. R., Simon, M., Brown, R. A., Zimmerman, N., Chabrier, G., & Baraffe, I. 2010, ApJ, 716, 1551
Lemke, M. 1989, A&A, 225, 125
Lloyd, J. P., Martinache, F., Ireland, M. J., Monnier, J. D., Pravdo, S. H., Shaklan, S. B., & Tuthill, P. G. 2006, ApJ, 650, L131
Malagnini, M. L., Faraggiana, R., & Morossi, C. 1983, A&A, 128, 375
Malo, L., Doyon, R., Lafrenière, D., Artigau, É., Gagné, J., Baron, F., & Riedel, A. 2013, ApJ, 762, 88
Marois, C., Doyon, R., Racine, R., & Nadeau, D. 2000, PASP, 112, 91
Marois, C., Lafrenière, D., Doyon, R., Macintosh, B., & Nadeau, D. 2006a, ApJ, 641, 556
Marois, C., Lafrenière, D., Macintosh, B., & Doyon, R. 2006b, ApJ, 647, 612
Mason, B. D., Wycoff, G. L., Hartkopf, W. I., Douglass, G. G., & Worley, C. E. 2001, AJ, 122, 3466
Mermilliod, J. C. 1997, VizieR Online Data Catalog, 2168, 0
Metchev, S. A., & Hillenbrand, L. A. 2009, ApJS, 181, 62

Monnier, J. D., Che, X., Zhao, M., Ekström, S., Maestro, V., Aufdenberg, J., Baron, F., Georgy, C., Kraus, S., McAlister, H., Pedretti, E., Ridgway, S., Sturmann, J., Sturmann, L., ten Brummelaar, T., Thureau, N., Turner, N., & Tuthill, P. G. 2012, ApJ, 761, L3
Morossi, C., & Malagnini, M. L. 1985, A&AS, 60, 365
Napiwotzki, R., Schoenberner, D., & Wenske, V. 1993, A&A, 268, 653
Nielsen, E. L., & Close, L. M. 2010, ApJ, 717, 878
Oppenheimer, B. R., Baranec, C., Beichman, C., Brenner, D., Burruss, R., Cady, E., Crepp, J. R., Dekany, R., Fergus, R., Hale, D., Hillenbrand, L., Hinkley, S., Hogg, D. W., King, D., Ligon, E. R., Lockhart, T., Nilsson, R., Parry, I. R., Pueyo, L., Rice, E., Roberts, J. E., Roberts, Jr., L. C., Shao, M., Sivaramakrishnan, A., Soummer, R., Truong, T., Vasisht, G., Veicht, A., Vescelus, F., Wallace, J. K., Zhai, C., & Zimmerman, N. 2013, ApJ, 768, 24
Oppenheimer, B. R., Beichman, C., Brenner, D., Burruss, R., Cady, E., Crepp, J., Hillenbrand, L., Hinkley, S., Ligon, E. R., Lockhart, T., Parry, I., Pueyo, L., Rice, E., Roberts, L. C., Roberts, J., Shao, M., Sivaramakrishnan, A., Soummer, R., Vasisht, G., Vescelus, F., Wallace, J. K., Zhai, C., & Zimmerman, N. 2012, in Society of Photo-Optical Instrumentation Engineers (SPIE) Conference Series, Vol. 8447, Society of Photo-Optical Instrumentation Engineers (SPIE) Conference Series, 844720–1
Oppenheimer, B. R., & Hinkley, S. 2009, ARA&A, 47, 253
Palmer, D. R., Walker, E. N., Jones, D. H. P., & Wallis, R. E. 1968, Royal Greenwich Observatory Bulletins, 135, 385
Patience, J., King, R. R., de Rosa, R. J., & Marois, C. 2010, A&A, 517, A76
Pickles, A. J. 1998, PASP, 110, 863
Prugniel, P., Soubiran, C., Koleva, M., & Le Borgne, D. 2007, ArXiv Astrophysics e-prints
Pueyo, L., Crepp, J. R., Vasisht, G., Brenner, D., Oppenheimer, B. R., Zimmerman, N., Hinkley, S., Parry, I., Beichman, C., Hillenbrand, L., Roberts, L. C., Dekany, R., Shao, M., Burruss, R., Bouchez, A., Roberts, J., & Soummer, R. 2012a, ApJS, 199, 6
Pueyo, L., Hillenbrand, L., Vasisht, G., Oppenheimer, B. R., Monnier, J. D., Hinkley, S., Crepp, J., Roberts, Jr., L. C., Brenner, D., Zimmerman, N., Parry, I., Beichman, C., Dekany, R., Shao, M., Burruss, R., Cady, E., Roberts, J., & Soummer, R. 2012b, ApJ, 757, 57
Racine, R., Walker, G. A. H., Nadeau, D., Doyon, R., & Marois, C. 1999, PASP, 111, 587
Rameau, J., Chauvin, G., Lagrange, A.-M., Klahr, H., Bonnefoy, M., Mordasini, C., Bonavita, M., Desidera, S., Dumas, C., & Girard, J. H. 2013, ArXiv e-prints
Reis, W., Corradi, W., de Avillez, M. A., & Santos, F. P. 2011, ApJ, 734, 8
Rice, E. L., Barman, T., Mclean, I. S., Prato, L., & Kirkpatrick, J. D. 2010, ApJS, 186, 63
Roberts, J. E., Dekany, R. G., Burruss, R. S., Baranec, C., Bouchez, A., Croner, E. E., Guiwits, S. R., Hale, D. D. S., Henning, J. R., Palmer, D. L., Troy, M., Truong, T. N., & Zolkower, J. 2012a, in Society of Photo-Optical Instrumentation Engineers (SPIE) Conference Series, Vol. 8447, Society of Photo-Optical Instrumentation Engineers (SPIE) Conference Series
Roberts, Jr., L. C., Rice, E. L., Beichman, C. A., Brenner, D., Burruss, R., Crepp, J. R., Dekany, R. G., Hillenbrand, L. A., Hinkley, S., Ligon, E. R., Lockhart, T. G., King, D., Metchev, S., Oppenheimer, B. R., Parry, I. R., Pueyo, L., Roberts, J. E., Shao, M., Sivaramakrishnan, A., Soummer, R., Vasisht, G., Vescelus, F. E., Wallace, J. K., Zimmerman, N. T., & Zhai, C. 2012b, AJ, 144, 14
Roeser, S., Demleitner, M., & Schilbach, E. 2010, AJ, 139, 2440
Samus, N. N., Pastukhova, E. N., & Durlevich, O. V. 2007, Peremennye Zvezdy, 27, 6
Santos, N. C., Melo, C., James, D. J., Gameiro, J. F., Bouvier, J., & Gomes, J. I. 2008, A&A, 480, 889
Schmidt-Kaler, T. 1982, Bulletin d'Information du Centre de Donnees Stellaires, 23, 2
Sivaramakrishnan, A., & Oppenheimer, B. R. 2006, ApJ, 647, 620
Smyth, W. H. 1844, A cycle of celestial objects
Soubiran, C., Le Campion, J.-F., Cayrel de Strobel, G., & Caillo, A. 2010, A&A, 515, A111
Soummer, R., Pueyo, L., & Larkin, J. 2012, ApJ, 755, L28
Steigman, G. 2010, JCAP, 4, 29
Stephens, D. C., Leggett, S. K., Cushing, M. C., Marley, M. S., Saumon, D., Geballe, T. R., Golimowski, D. A., Fan, X., & Noll, K. S. 2009, ApJ, 702, 154
Tagliaferri, G., Cutispoto, G., Pallavicini, R., Randich, S., & Pasquini, L. 1994, A&A, 285, 272
Torres, C. A. O., Quast, G. R., Melo, C. H. F., & Sterzik, M. F. 2008, Young Nearby Loose Associations, ed. B. Reipurth, 757
Townsend, R. H. D., Owocki, S. P., & Howarth, I. D. 2004, MNRAS, 350, 189
Valenti, J. A., & Fischer, D. A. 2005, ApJS, 159, 141
van Belle, G. T., van Belle, G., Creech-Eakman, M. J., Coyne, J., Boden, A. F., Akeson, R. L., Ciardi, D. R., Rykoski, K. M., Thompson, R. R., Lane, B. F., & PTI Collaboration. 2008, ApJS, 176, 276
van Leeuwen, F., ed. 2007, Astrophysics and Space Science Library, Vol. 350, Hipparcos, the New Reduction of the Raw Data
Viana Almeida, P., Santos, N. C., Melo, C., Ammler-von Eiff, M., Torres, C. A. O., Quast, G. R., Gameiro, J. F., & Sterzik, M. 2009, A&A, 501, 965
Vigan, A., Patience, J., Marois, C., Bonavita, M., De Rosa, R. J., Macintosh, B., Song, I., Doyon, R., Zuckerman, B., Lafrenière, D., & Barman, T. 2012, A&A, 544, A9
Wahhaj, Z., Liu, M. C., Biller, B. A., Clarke, F., Nielsen, E. L., Close, L. M., Hayward, T. L., Mamajek, E. E., Cushing, M., Dupuy, T., Tecza, M., Thatte, N., Chun, M., Ftaclas, C., Hartung, M., Reid, I. N., Shkolnik, E. L., Alencar, S. H. P., Artymowicz, P., Boss, A., de Gouveia Dal Pino, E., Gregorio-Hetem, J., Ida, S., Kuchner, M., Lin, D. N. C., & Toomey, D. W. 2011, ApJ, 729, 139
Wallace, J. K., Green, J. J., Shao, M., Troy, M., Lloyd, J. P., & Macintosh, B. 2004, in Advancements in Adaptive Optics. Edited by Domenico B. Calia, Brent L. Ellerbroek, and Roberto Ragazzoni. Proceedings of the SPIE, Volume 5490, pp. 370-378 (2004)., ed. D. Bonaccini Calia, B. L. Ellerbroek, & R. Ragazzoni, 370–378
Westin, T. N. G. 1985, A&AS, 60, 99
Wilson, R. E. 1953, Carnegie Institute Washington D.C. Publication, 0
Wu, Y., Singh, H. P., Prugniel, P., Gupta, R., & Koleva, M. 2011, A&A, 525, A71
Zacharias, N., Finch, C. T., Girard, T. M., Henden, A., Bartlett, J. L., Monet, D. G., & Zacharias, M. I. 2012, VizieR Online Data Catalog, 1322, 0
Zhai, C., Vasisht, G., Shao, M., Lockhart, T., Cady, E., Oppenheimer, B., Burruss, R., Roberts, J., Beichman, C., Brenner, D., Crepp, J., Dekany, R., Hinkley, S., Hillenbrand, L., Ligon, E. R., Parry, I., Pueyo, L., Rice, E., Roberts, L. C., Sivaramakrishnan, A., Soummer, R., Vescelus, F., Wallace, K., & Zimmerman, N. 2012, in Society of Photo-Optical Instrumentation Engineers (SPIE) Conference Series, Vol. 8447, Society of Photo-Optical Instrumentation Engineers (SPIE) Conference Series
Zimmerman, N., Brenner, D., Oppenheimer, B. R., Parry, I. R., Hinkley, S., Hunt, S., & Roberts, R. 2011, PASP, 123, 746
Zimmerman, N., Oppenheimer, B. R., Hinkley, S., Brenner, D., Parry, I. R., Sivaramakrishnan, A., Hillenbrand, L., Beichman, C., Crepp, J. R., Vasisht, G., Roberts, L. C., Burruss, R., King, D. L., Soummer, R., Dekany, R., Shao, M., Bouchez, A., Roberts, J. E., & Hunt, S. 2010, ApJ, 709, 733
Zorec, J., & Royer, F. 2012, A&A, 537, A120
Zuckerman, B., Rhee, J. H., Song, I., & Bessell, M. S. 2011a, ApJ, 732, 61
—. 2011b, ApJ, 732, 61
Zuckerman, B., & Song, I. 2012, ApJ, 758, 77